CRITICAL MATERIAL PARAMETERS FOR MODELING DEVICES MADE FROM AN EPOXY-BASED SHAPE MEMORY POLYMER

A Thesis

by

VEYSEL EREL

Submitted to the Office of Graduate and Professional Studies of
Texas A&M University
in partial fulfillment of the requirements for the degree of

MASTER OF SCIENCE

Chair of Committee,	Terry Creasy
Committee Members,	Arun Srinivasa
	Nguyen Hung
Head of Department,	Andreas A. Polycarpou

August 2014

Major Subject: Mechanical Engineering

ABSTRACT

Differential scanning calorimetry (DSC), simple tension, and planar tension experiments were used to investigate the behavior of an epoxy-based shape memory polymer (SMP) system. DSC results found the mixture had consistent glass transition at 70° C, which agreed with prior research with this formulation.

Simple tension experiments were consistent with nonlinear elastic behavior and FEA analysis agreed with the experiments. However, the nonlinear elastic model did not predict the performance found in planar tension.

Planar tension results were unexpected. The stress/strain response was sigmoidal with a significant plateau in stress followed by rising stress to failure. The standard 10:1 gage width/gage length ratio seemed to over constrain the material. The strain to failure was small, and insufficient for extracting hyperelastic parameters. Using narrower gage width specimens, or perhaps a new specimen design, would benefit modeling and analysis for this material.

ACKNOWLEDGEMENTS

I would like to thank my chair, Dr. Terry S. Creasy for his guidance, encouragement, and support throughout this research. Dr. Creasy likes to spend time with his students and wants to teach everything that he knows. Each meeting Dr. Creasy tells his experiences about life and research until we get the main idea. I also want to thank my committee members, Dr. Srinivasa for his interesting ideas about shape memory polymer and Dr. Liang for his feedback.

I also would like to thank my friends, Jessica Berry and Nitin Suarez, for teaching me manufacturing SMP, giving permission to use chemical engineering laboratory, and advising me when I encountered with problems. The other person that I am grateful is Blake Teipel for giving invaluable advice and sharing his experiences.

Finally, I would like to thank my mother, father, sister and brother for their encouragement and support although they live twelve thousand miles away from Texas. They always trusted me for my critical decisions during my life.

NOMENCLATURE

ABS	Acrylonitrile Butadiene Styrene
AFO	Ankle-Foot Orthosis
ASTM	American Society for Testing and Materials
DIC	Digital Image Correlation
DMA	Dynamic Mechanical Analysis
DSC	Differential Scanning Calorimetry
FEA	Finite Element Analysis
NGDE	Neopentyl Glycol Diglycidyl Ether
RP	Rapid Prototype
SMP	Shape Memory Polymer
T_g	Glass Transition Temperature

TABLE OF CONTENTS

Page

LIST OF FIGURES

LIST OF TABLES

1. INTRODUCTION

1.1 Motivation

Prosthetics such as artificial limbs facilitate a disabled person's life. Patients can remain ambulatory, perhaps even run. Paralympic games show that athletes with prosthetics can run or perform in sports. Prosthetic limbs attach to the wearer by a socket that accepts the residual limb. The socket material should be carefully considered to withstand everyday activities and—if the person desires—running and jumping. Prosthetists must consider that the user's weight and motions may cause high load in the socket. Figure 1 shows a prosthetic limb with an artificial socket. [1- 4]

Figure 1. This prosthetic limb shows a typical orthopedic socket. [5]

Composite materials have properties that make them interesting for orthopedic and prosthetic devices. [1] Composite materials are two or more constituents with disparate physical and chemical properties that are combined intentionally to obtain novel material properties. [2, 3] Fiber-reinforced polymer composites are widely used multiphase materials in orthopedics. [1]

High strength and moderate elastic modulus are prerequisites for artificial limb materials because the user's actions generate significant loads and the artificial limb must match the stiffness typical for a natural limb. [1] The socket's interior surface quality is also vital for comfort and controllability. [1]

Traditional ankle-foot orthosis (AFO) fabrication is inconvenient [6]. Orthoses are custom fit to each person because each person's leg has a unique shape. Patients must visit a clinic at least 3 times for their fitting. Practitioners need to reduce labor and fabrication time. Morrison et al., [6] suggested making AFOs using mass production with a final adjustment in shape made during fitting.

Morrison's work provides inspiration for the present project. Orthopedic sockets must be custom fit. In addition, socket fabrication and adjustments are expensive. If the socket does not fit limb correctly, specialists might scrap socket and introduce a high cost in labor, time, and materials. This thesis considers shape memory polymer (SMP), which have growing use for biomedical applications, as the matrix that will enable post-forming of prosthetic sockets. This work will determine the fundamental characteristics and limits for an SMP material and the effect that SMP behavior has on design.

1.1.1 SMPs and Their Applications

Shape Memory Polymer (SMP) is a shape-memory material subclass that exhibits soft and hard material behavior depending on the stimulus. Thermally induced SMP—when heated above its glass transition temperature (T_g)—can be shaped into a new conformation, or, if the material is unrestrained, return to its initial conformation. [7] More details about SMP and its response appear in Chapter 2.

SMP research has increased in the last decade because its initial shape can be changed and recovered. Potential SMP applications range from simple adjustable kitchen utensils, to tools, [8] actuators, [9-12] temperature sensors, [13-16] and biomedical devices such as biodegradable, self-tightening sutures, [17-18] and self-expanding stents. [19-20] SMPs have several excellent properties: lightweight, low cost, fabrication ease, and high recoverable strain. [21] These features make them a good option for some components. Shape memory materials bring a new perspective to device design from prosthetics to aircraft structures. When designing a device, one should consider three primary SMP characteristics:

Shape fixity: the shape retained after the material cools below the T_g.

Shape recovery: the shape obtained after raising the material above its T_g and allowing it to revert freely toward its initial shape.

Recovery stress: the stress the SMP generates when heated above its T_g while fixed in the deformed shape.

Figure 2 shows cycle from initial shape to initial shape that has shape recovery and shape fixing behavior. More detailed information and formulas that help to determine shape fixity and recovery appear in the SMP characterization methods section.

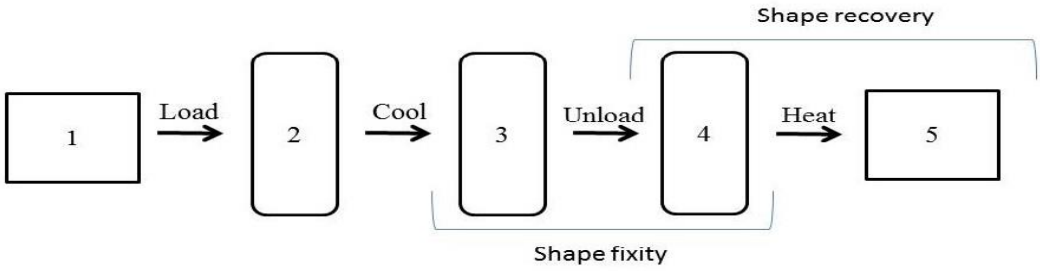

Figure 2. Shape fixity and recovery response can obtain different steps.

Each SMP response can accomplish something in a device. Shape fixity allows a standard spoon to become a custom spoon with a handle shaped for a specific person. While hot, it can assume the user's hand shape. At room temperature, it can hold the new shape to provide easy use and comfort. [22] Shape recovery supports folded structures that deploy easily and return from a stored shape to their functional shape. For example, folded or compressed implants can enter the human body through a small incision. After the implant passes through a guide tube, it is unloaded and body temperature returns the implant to its functional shape. [21, 23] Figure 3 shows shape changing stents. Smart surgical sutures that help to close a wound might employ SMP's stress recovery response.

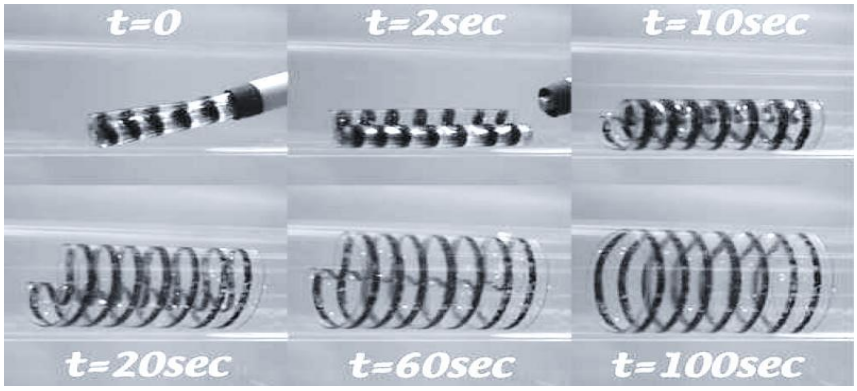

Figure 3. After load is removed from an SMP stent, the stent recovers. Black lines drawn around the stent make the shape change clear. [24]

Current, mass produced SMPs are foils and cables. The automobile industry used SMP to manufacture automotive choke systems before electronic injection was practical. Figure 4 shows a mandrel for filament winding covered with Kevlar filament; mandrels must change shape so that workers can remove them from the cured composite part. SMP can fold into a small shape for extraction and recover to the mandrel shape after heat treatment. These mandrels are reusable. [25]

Figure 4. Reusable mandrel covered by filament. [30]

In aeronautics, the SMP-based morphing wing structure appearing in Figure 5 is a candidate for advanced wings. [29] Morphing wings would alter their wing shape to match each flight phase. By doing that, energy loss from air friction in flight would decrease and save fuel. Use of SMP is growing in aerospace. Deployable satellite antennas and sun-sails are popular SMP applications. [26, 27] SMP is desirable in space because sunlight is the only power source needed to deploy the structure. [28] Figure 6 shows a deployable reflector made of SMP composites.

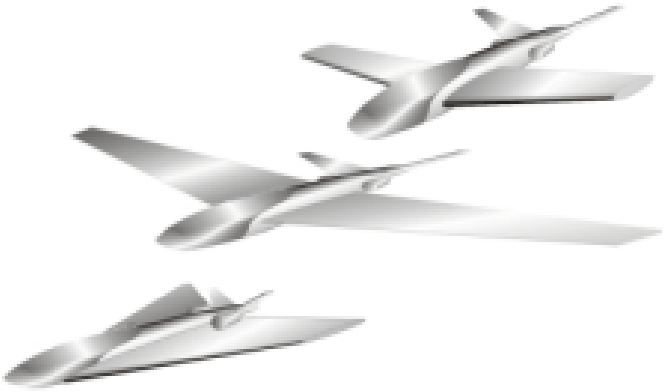

Figure 5. Plane morphing wing would open and close during the flights. [31]

SMP's phase transition from glassy solid to rubbery solid changes the material's diffusivity, transparency, and mechanical properties. These reversible changes help make SMP useful in smart fabrics that are waterproof, yet breathable. [7,32,33] During cold weather, fabrics become impermeable and contain body heat. In contrast, in hot weather permeability increases and the fabric releases body heat. [34]

Figure 6. SMP composite reflector in the hybrid inflatable antenna. [35]

Many researchers are looking into SMP medical applications. Two essential characteristics attract scientists' attention. Great biocompatibility, which is a crucial property, pushes researchers to develop more SMP components. [21] The second desirable characteristic is tailoring the glass transition temperature (T_g) for each application. SMPs can exhibit targeted T_g for shape recovery and self-deployment inside or outside of the body.

Hayashi et al. are researching medical SMP applications. One experiment tried catheters that have high stiffness at ambient temperature and become soft and more suited for use inside the body. This group considered using SMP materials in orthopedics and dentistry. Furthermore, they stated that in the glass transition region

SMP has a very smooth feel that is similar to human skin. Thus it could use for body contact side of artificial devices or implants. [21]

Minimally invasive surgery is in high demand because the patient loses less blood, has less post-operation pain, and has smaller scars. [36,37] Closing incisions with sutures and tying a knot is difficult. [38] If the proper stress is not applied to get the wound lips closed, necrosis and hernias may occur. Figure 7 shows a smart suture tightening as temperature increases. [39] This smart surgical suture, which contracts and tightens the knot when exposed to body temperature, might be better closure. [17]

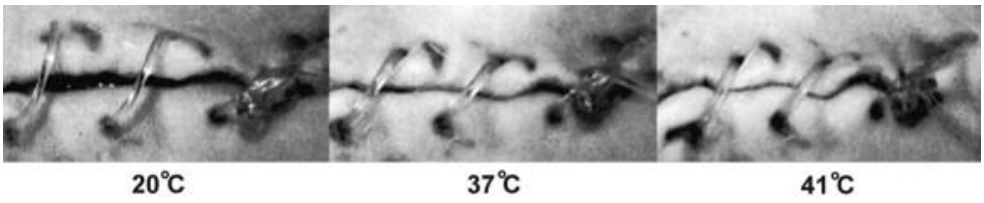

Figure 7: Degradable shape-memory suture for wound closure. These photos come from an animal experiment. [17]

1.2 Objective

This thesis has a primary purpose: characterize an epoxy-based shape memory polymer using standard mechanical tests for elastomers and determine if these parameters are essential for designing SMP based devices.

No prior study has characterized epoxy-based shape memory polymer made from Epon 826, Diamine, and (Neopentyl glycol diglycidyl ether) NGDE components as an elastomeric system. The fundamental question is whether epoxy-based SMP in the rubbery state requires three dimensional parameters deformation parameters successful

design. This work will determine those constants and apply them to simple device that exhibits large deformations when the SMP is above its glass transition temperature.

2. LITERATURE REVIEW

2.1 Shape Memory Polymers

Stimuli responsive polymers and smart polymer can respond to environmental changes. These polymers can identify a stimulus as a signal, judge signal's magnitude and rearrange their chain conformation toward the response. [21] Stimulus might be not only temperature, light, electrical field, but also pH, chemical agents and ionic factors. Between these, temperature is the most widely used stimulus. [7] The response demonstrates itself as a shape, color, reflective index and permeability change. [22]

Actively moving polymers, which respond with shape change, are a subset of smart polymers. These polymers fall into two sub-classes. One subclass is shape-changing polymers that change their shape while exposed to a stimulus. Once the stimulus stops, the material returns to its original shape. [40]

The second active moving polymer is shape memory polymer (SMP), which can maintain its temporary shape if that shape is held until the temperature falls below the material's T_g. [40]

SMPs are unique because they have these properties and advantages:

- Exhibit more than 400% strain
- Have very good biocompatibility
- Tailorable glass transition temperature, which provides wide use range, -70 C to 70 C.
- Low density than metals

- Good damping near T_g
- Manufacturable, feasible to mold, extrude and machine.
- Lower cost than shape memory alloys. [7]

SMPs have been studied since 1980's. One SMP with considerable interest is the thermally responsive systems based on epoxy. [7] The response and the resulting mechanical properties before, during, and after shape change are the focus for the present research.

Thermally responsive or thermally induced SMPs can change their shape quickly and easily above the transition temperature (T_{trans}) and shape stabilize when they are below this temperature. Once they are re-exposed to heat that is above (T_{trans}), they return to their previous shape. [7] Transition temperature may have different meanings according to polymer crystallinity. If the polymer is amorphous (non-crystalline solid)$T_{trans} = T_{glass}$, or polymer is in a crystalline state $T_{trans} = T_{melting}$. [8] The melting phenomenon could determine the transition temperature. If sharper transition observed during melting process, it means $T_{trans} = T_{melting}$. [43] This transformation, which is elaborately described next paragraph, appears in Figure 2.

First, the material gets an initial shape during curing and fabrication. Then, the material reaches a rubbery state when heated about the glass transition temperature. Second, a load changes the materials shape. The load remains as the material cools below the T_g. Once heat falls below transition temperature, the material tends enters the glassy state. Polymers exhibit rubbery behavior above T_g and glassy behavior below glass transition temperature. Elastic modulus in a glass state is at least two times or at

most five hundred times larger than elastic modulus in rubbery state. [5] Between the third and fourth steps, the load is removed and the material cannot reverse deformation because the glassy state locks the polymer chains into the new configuration. Finally, heated above T_g the material becomes rubbery and—if not under load—reverts to its permanent shape. [44]

Kelch and Lendlien explained the transformation morphology. [8] Polymer segment motion freezes in the glassy circumstance. Changing from glassy state to rubbery state happens when thermal activation that frees the segments from their secondary bonds. This unhindered condition helps the segments move toward an energetically favorable conformation, that is, a lower energy state. However, entanglements restrict the move toward the low energy state. If drawing stress acts for a short time, entanglements impede large chain displacement and the specimen returns to its previous shape when the load stops. On the other hand, if high tensile stress acts for a long time, chains slip and disentangle from each other. Therefore, the polymer cannot return to its previous shape. In this way, increasing temperature above glass transition temperature causes increasing chain mobility and decreasing elastic modulus. [45, 46]

Most SMP studies used one-step SMP that remembers one shape: their initial, i.e., permanent shape. These can hold many temporary shapes, but they return to the same shape each time. [47-49] there are also multiple-shape and multiple-step SMPs for complex applications. [50] These “stepwise” SMPs have two or more remembered shapes. A stepwise SMP material appears in Figure 8. Li at al [51] created a four step

SMP that has two transition temperatures. They used polymethlymetacrylate/ polyethylene glycol that supplies extensive T_g.

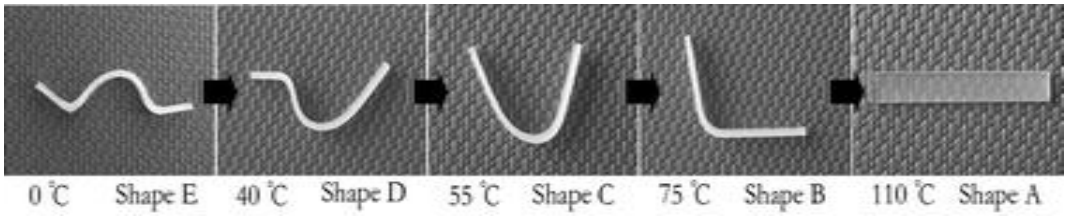

Figure 8: Four-step shape memory effect can be observed with different temperature. [34]

2.2 Epoxy Shape Memory Polymer

SMPs fall into two groups: thermoplastics and thermosets according to their structures. Thermoplastic SMPs lack physical cross-links and that means molecule-molecule interaction is intermolecular by entanglements or secondary bonds. Thermoplastics can be amorphous or semi crystalline and they melt. On the other hand, thermoset SMPs have chemical cross-links that are covalently bound. Therefore, these materials cannot melt—thermosets decompose at elevated temperature. Thermosets have higher moduli; greater thermal, chemical, and dimensional stability; and better environmental durability than thermoplastics. [52,53]

Physically and chemically cross-linked SMPs have been studied for twenty years. Most physically cross-linked SMPs use polyurethane chemistry. Polyhedral oligomeric silsesquioxane-polyethlene glycol [54,55], aramid-polycaprolactone [56], nylon 6-polyehylene [57,58] are some of the physically cross-linked structure with shape memory effect. Scientist developed chemically cross-linked SMPs to achieve perfect

mechanical properties, various transition temperature and enhanced shape memory performance.

Epoxy resin is the most popular thermoset. Researchers has been paying more attention epoxy based SMPs due to good shape memory performance. [59] In addition to shape memory, epoxy can be formulated for different requirements.

This thesis covers epoxy-based shape memory polymer. Xie found a good mixture that produced shape memory material. [60] He showed that either decreasing crosslink density or increasing chain flexibility decreased T_g. Chain flexibility affects glass transition temperature strongly. He added NGDE in several, increasing concentrations to increase chain flexibility and decrease crosslink density. He obtained a wide glass transition temperature. Rimduist and Lohwerathama [61] analyzed the effects benzoxazine resin has on thermal and mechanical properties. Benzoxazine resin is enriched epoxy resin. It has more has more amine bounds than epoxy resin. They used Jeffamine and NGDE to make SMP like Mister Xie did.

Rousseau [62] examined various shape memory epoxies to provide different properties. Two epoxy resins, Epon 826 and Epon 828, two Jeffamines cure agents, D230 and T403, and Neopentyl glycol diglycidyl ether (NGDE) were mixed in different percentage combination to vary T_g and material properties. They used Thermo-mechanical analyzer to obtain shape memory behavior for consecutive cycles. They used a high temperature cyclic test. They applied 7 percent strain and recorded 21 cycles. In this thesis, high temperature cyclic test run to obtain similar results. Chapter 4 covers these chemicals in more detail.

Material science researchers have measured thermomechanical properties of SMPs. The suite of experiments includes tension below T_g; tension above T_g; flexural stiffness and strength; compression; and planar tension above T_g.

2.3 Review of Epoxy Shape Memory Polymer Characterization

Characterizing a material's performance is critical to understanding the material and to applying the material. This section explains several characterization methods that help us understand these materials.

The fold-deploy experiment determines shape fixity ratio and shape recovery ratio. First, the specimen is heated twenty to thirty degrees centigrade above T_g. Then, it is bent into a U shape to determine maximum bending angle (Q_{max}). Third, the specimen is cooled while held in the U shape and until the specimen is under its T_g. Without the external load, the sample exhibits slight elastic shape changes that set Q_{fixed}. Finally, the sample is heated and allowed to freely recover and then Q_{end} is measured. These fixity and recovery ratios come from these formulas:

Shape retention ratio (R_f) = $\frac{Q_{fixed}}{Q_{max}} \times 100\%$ [63]

Shape recovery ratio (R_r) = $\frac{Q_{max}-Q_{end}}{Q_{max}} \times 100\%$ [64]

where Q_{max} is maximum bending angle, Q_{end} is bending angle when recovery ends and Q_{fixed} is angle after the load is removed.

Wei and Zhu [53] and Liu [65] investigated shape memory properties with the U bending test. They varied the epoxy resin and curing agent to influence the crosslink

density. Although this can be done with complicated thermomechanical cyclic tests, but, fold-deploy tests are easy to run.

Several researchers define recovery rate as the shape transformation speed for a shape recovery that starts from the temporary shape and obtains the permanent shape. Liu [65] named it “speed recovery process;” however, others call this test “deformation recovery speed” and “shape recovery speed”. [7]

Dynamic Mechanical Analysis (DMA) is a good technique for measuring material thermomechanical properties. Applied cyclic load—tensile, flexural, or compressive—stimulates the stress/strain behavior over a temperature range. Glass transition temperature, loss and storage moduli, and phase angle come from this test.

Mechanically characterizing epoxy SMPs is crucial. The tensile test is a common starting point. Wei and Zhu [53] measured epoxy resin material tension and three-point bending behavior at room temperature. Various percentages of hydro epoxy resin were mixed with polypropylene glycol and diglycidyl ether to determine their influence. They concluded that T_g and crosslinked density decreased as the NGDE volume ratio increased.

Fulcher and Karaca et al. [52] used Veriflex-E thermoset epoxy resin. They did large scale compression and small-scale indention test to examine compressive properties of SMPs. Shape recovery test were also run for different conditioned samples. Compression results stiffness range is wider than tensile according to their results. Additional experiments were done to understand different environmental effect by exposing samples to water, oil and UV radiation. Unconditioned specimen exhibits

highest properties. Study concluded that environment conditions effects glass transition temperature, mechanical properties and shape recovery capabilities. Rimdusit and Lohwerathama [61] used benzoxazine-modified epoxy to produce SMP. Flexural test, shape recovery test was run to obtain mechanical properties. Outcome of experiment is modified epoxy flexural strength and flexural modulus higher than unmodified epoxy.

Liquid takes the shape of container when they freeze. When epoxy mixed with curing agent, it takes the shape of the container. Mechanical tests need specific specimen shape. Therefore, specific molds needed to produce specimen. Next Chapter was mentioned about specimen fabrications and materials.

3. MATERIALS AND FABRICATION

3.1 Shape Memory Epoxy Polymer

3.1.1 Epoxy Resin

Epoxy resin used for producing specimens is diglycidyl ether of biphenyl A epoxy monomer. It is also called 2,2-bis(4-hydroxphenyl) propane, 4,4'-Isopropylidenediphenol diglycidyl ether. Figure 9 shows this molecule's chemical structure. Known with commercially as EPON 826 and abbreviated to DGEBA. Epichlorohydrin, two moles, and bisphenol A, one mole, react to form this molecule. [66] The EPON was bought from Momentive Company and used right after delivery.

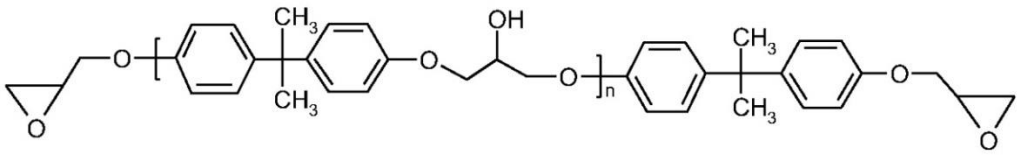

Figure 9. Epon 826 has this chemical structure with equal to 0.085. Because n<<1, EPON 826 is a low viscosity resin.

This material has broad application in reinforced pipes, adhesives for electrical and aerospace, tooling constituents, and flooring. Low viscosity and lightly colored, it reacts with various curing agents to provide good properties. [67]

Low viscosity is important for processes like filament winding, pressure laminating, and spraying. During fiber-reinforced pipe fabrication, low viscous resistance provides quick wetting for glass, boron, and aramid fibers. Low viscosity

helps to fill voids too. In addition, cured EPON 826 has low electrical conductivity that makes it popular as an insulating encapsulation. [67]

3.1.2 Diamine (D230)

Diamine (D230) is a quad-functional amine cure agent that cures EPON 826 at room temperature. O,O'-Bis (2-aminoproplypropylenne glycol and Polypropylene glycol 130 bis(2-aminoproplypropyl ether) are diamine chemical names. Commercial name used by Huntsman is Jeffamine D230. It is formed by oxypropylene replication unit in the backbone structure. Chain structure has amine group either chain side.[68] Figure 10 shows Oxypropylene and Diamine chemical structure. N is equal to 2.5.

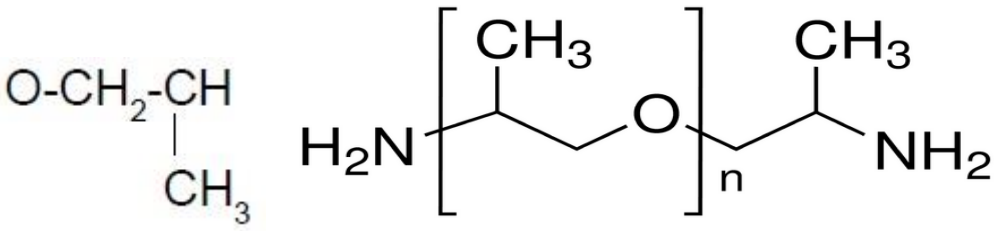

Figure 10. Oxypropylene and Diamine D-230

Low viscosity, low vapor pressure and perfect miscible with many solvents are good properties. It offers good resistance to coatings and adhesives.

3.1.3 Neopentyl Glycol Diglycidyl Ether (NGDE)

Neopentyl glycol diglycidyl ether is colorless, liquid component of epoxy based SMPs [70]. NGDE, a flexible aliphatic diepoxide, replaces some EPON 826 to increase chain flexibility. Changing chain flexibility affects the glass transition temperature.

Because NGDE has a lower equivalent weight than EPON, substitution EPON for NGDE raises the crosslink density [71]. NGDE was bought from TCI America and it was used as-received. Figure 11 shows NGDE chemical structure, oxirane rings on the edges can connect to Diamine.

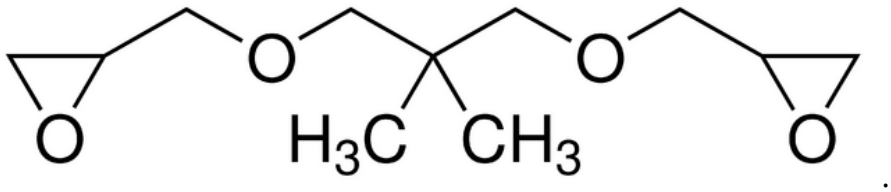

Figure 11.NGDE chemical structure has methyl group at structure center.

Among these three components (EPON, Jeffamine, NGDE) two reactions occur for every amine group. Primary epoxy resin oxirane ring (△) is opened and after this reaction aminoalcohal is produced. Figure 12 shows the steps the reaction takes. Every NH_2 need to react two oxiranes that epoxy resin and NGDE has in their structure. [69]

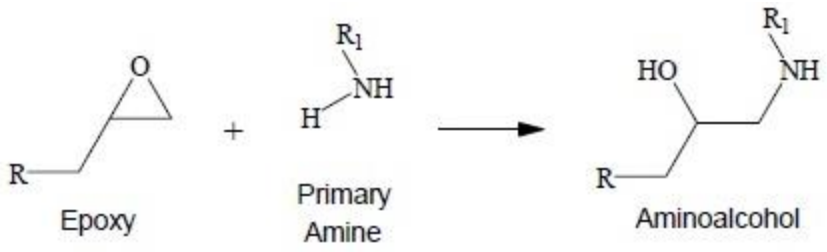

Figure 12. Oxirane ring breaks to interact with epoxy.

After first step, there is a still one available hydrogen in amino group that can react with the epoxy resin or NGDE. Because epoxy resin and NGDE have an oxirane ring in both sides, they can react and connect to four places on the backbone. Figure 13 shows reaction's second step. Second NH bond breaks and it connects to either epoxy or NGDE. [69]

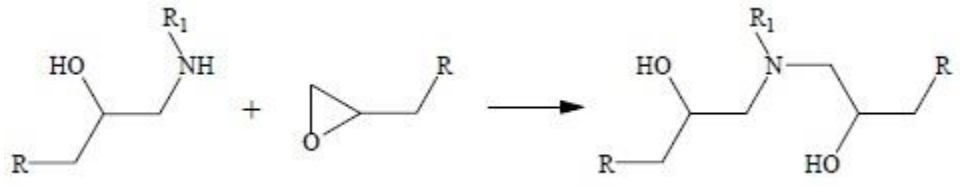

Figure 13. Oxirane ring can connect epoxy and NGDE.

3.2 Specimen Fabrication

3.2.1 Design Specimen

SMPs that deform above their glass transition temperature are operating in the rubbery region; therefore, the American Society for Testing and Materials (ASTM) test methods for elastomers provided insight into specimen design.

Manufacturing process starts with designing specimen. First, Solidworks 2013 software was used to draw 3D specimen model. Second, Design the silicone mold by subtracting specimen model. Third, design the RP mold subtracting silicone mold.

Making specimen process begins with, building negative mold by using rapid prototype (RP) machine. Second fill these molds with silicone and Finally, Cast the epoxy specimen into the silicone mold and wait for curing. Once cured, specimens are ready to run for experiment.

ASTM D0638-10 showed good practice tensile specimen designs. The Type V specimen is a short specimen that easily fits in the Instron's oven. This was a conservative choice that assured that specimen would fail before the fixtures hit the oven's top side during a high temperature test. Table 1 displays Type V dimensions in the Solidworks design.

Table 1. This table lists the dimensions of the ASTM Type V specimen.

Width of narrow section (W)	3.18 ± 0.4 mm
Length of narrow section (L)	9.53 ± 0.08 mm
Gage length (G)	7.62 ± 0.02 mm
Distance between grips (D)	25.4 ± 5 mm
Radius of fillet (R)	12.7 ± 0.08 mm

Figure 14 shows the specimen based on the measurements in Table 1 tensile specimen to scale.

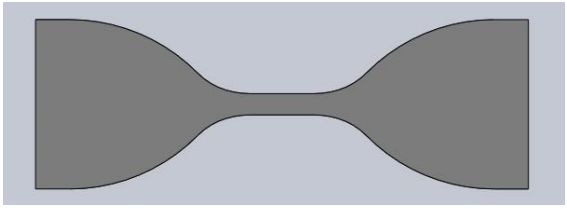

Figure 14. Tensile specimen solidworks drawing based on ASTM 638 standards.

With the specimen available as a 3D model, it was simple to design a silicone rubber mold that could hold six SMP tensile specimens. Epoxy based SMPs needs high

temperature curing, thus freeman silicone was chosen for specimen fabrication An assembly file held a block of virtual silicone and six tensile specimen models. The silicone block was edited in the assembly and the tensile specimens were subtracted, which left tensile specimen openings in the block. Finally the silicone mold model was aligned with a virtual ABS plastic block in a second assembly file. After the silicon mold was subtracted, the ABS block became a 'negative' mold. It is a secondary mold that allows forming the primary mold that forms the SMP into tensile specimens. Figure 15 shows the silicone and ABS molds as images within Solidworks.

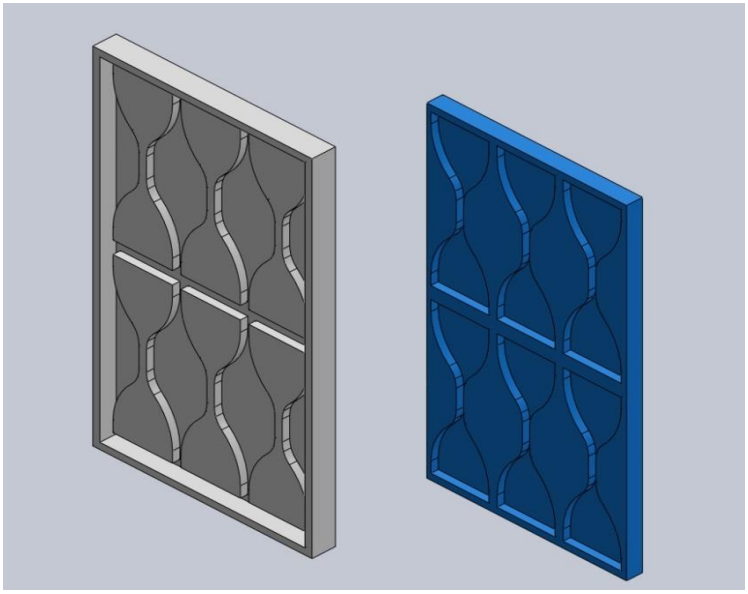

Figure 15. Drawing on the left shows ABS mold and drawing on the right shows silicone mold solidworks drawings.

The same process lead to the planar tension specimen mold design. The planar tension-pure shear specimen must have a large aspect ratio, that is, the specimen width divided by gage length must be 10 or greater, to produce a good pure shear effect within

minimal load from the extreme specimen edges. Considering the size limits imposed by Instron's environmental chamber, this planar tension specimen has a 10:1 aspect ratio with a 15 mm gage length. Specimen, rapid prototyping negative mold and silicone mold Solidworks images appear in Figure 16 and Figure 17.

Figure 16. Planar tension specimen dimensions

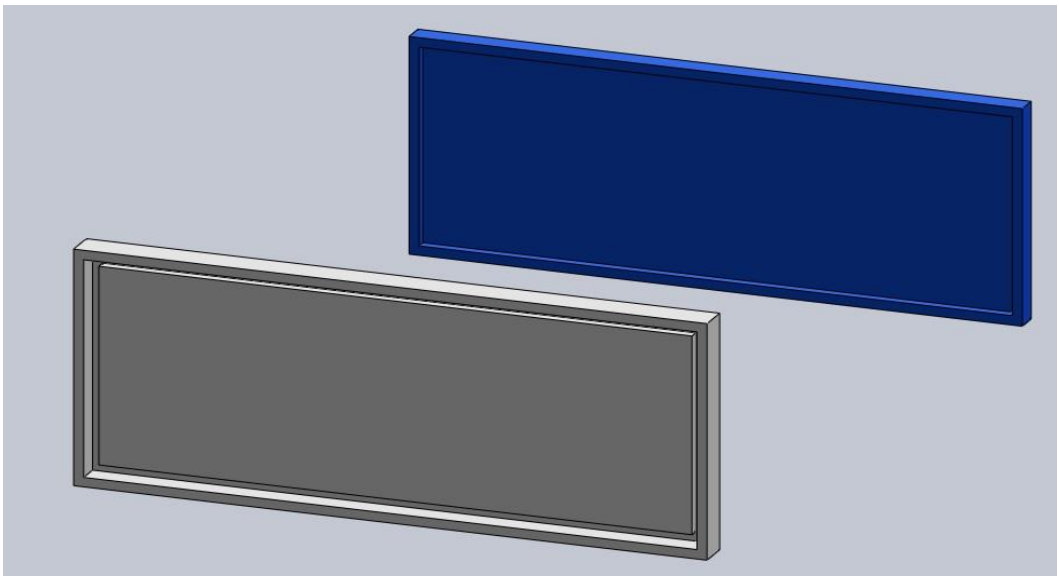

Figure 17. Front drawing shows abs mold and back drawings demonstrates planar tension silicone mold.

3.2.2 Rapid Prototype Negative Mold

Once the mold was defined, Solidworks wrote the shape information into a stereo lithography file (STL). Rapid prototyping mold was export to STL file to use it CatalysEX software for RPM. Solid works export options by way of fine resolution helps to observed material stress concentration. RP machine has an ability to build any shape by using different material. The machine that we have in our lab brand is BST 1200. It uses Acrylonitrile butadiene styrene (ABS) to generate parts. Material was supplied from Statasys –Ltd. Working principle of RP machine is like 3D printer. First it develop base with support material which helps to stick abs material. And then RPM starts to build parts that get drawings from software. The machine draws part layer by layer which causes surface roughness and voids on the surface. In Figure 18 there are some blue areas. Liquid silicone entered into the ABS molds because of the surface void. There is no effects were observed due to blue areas.

Figure 18. Tensile specimen and planar specimen ABS molds

Additional sanding process was applied to obtain smooth surface. Two different ways were found to obtain good surface. First method is vaporizing acetone melts surface, however it may cause loss of dimensional tolerance. Second method is using different sanding paper with different grits. Three different sanding papers were used to sand ABS molds. Figure 19 demonstrates 150,320 and 600 grit sand papers that were applied to mold respectively. Sand papers were adhered to small metal parts to distributed applied load homogeneously. Figure 20 shows 150 grit sand paper with small metal parts. Same number of sanding cycle were applied every mold section to achieve flat surfaces.

Figure 19. From the front to the back 150,320,600 grit sanding papers can be seen.

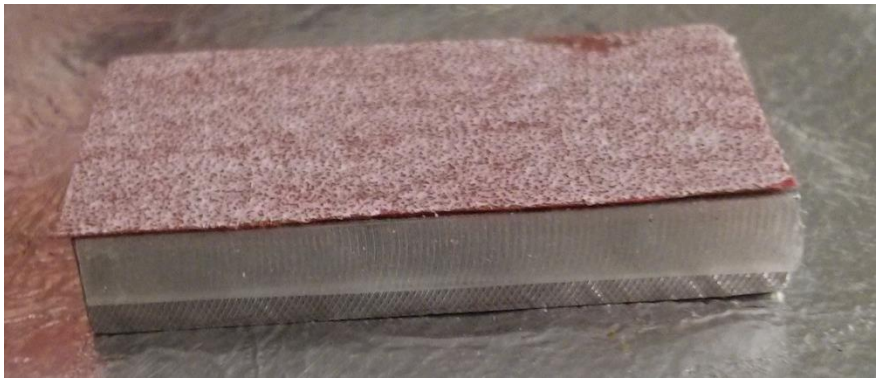

Figure 20. Sand papers attached to small metal part.

3.2.3 Casting Silicone Molds

After obtaining smooth ABS molds, the silicone mold was cast. Bluesil V-330 silicone elastomer (Freeman Manufacturing and Supply Company) came with two components. Mixing ratio by weight is 10:1 of part A and part B, respectively Specific gravity, which is 1.3, was entered into Solidworks to automatically calculate the mold's mass. Total mass was multiplied by 1.2 to cover loss during mixing and pouring. Table 2 shows A and B weights for tensile and planar silicone mold.

Table 2. Silicone mold components for tensile and planar tension mold

	Tensile Mold	Planar Tension Mold
Component A	106.6 gr	77.80 gr
Component B	10.6 gr	7.8 gr

After calculation usage of components, they were mixed in mixing cups. They degassed thirty minutes at high pressure to avoid bubbles in mold. End of the degassing

process, liquid silicone was poured to abs negative mold to obtain intended shape. The silicone cured for 20 hours before demolding. Exactly same process used for producing planar tension mold.

3.2.4 Process Epoxy Based Shape Memory Polymer

Processing SMP took five steps: dispensing constituents, mixing, degassing, pouring, and curing. The following paragraphs explain each step.

Epoxy resin, NGDE and Diamine (D-230) were dispensed at room temperature. EPON 826 is too viscous at room temperature. First, EPON was place into a 25 ml glass bottles by using stirring rod and then it heated on hot plate until it has low viscosity Figure 21 shows epoxy warming on the hot plate. After measuring hot EPON with a graduated cylinder, the EPON was placed in a 25 ml bottle. NGDE and Diamine were also put in to 25 ml bottles before mixing. Figure 22 shows the measure components ready for mixing. Bottles should be closed with caps to protect interaction between constituents to carbon dioxide and oxygen.

Figure 21. Epoxy is heating on hot plate.

Figure 22. Measured components were put in small class tubes before mixing all together. Covers were marked with their names.

Constituent mole numbers were obtained from Xie paper. [60] Table 3 demonstrates components chemical ratio volumes.

Table 3. Components volume ratio

Epon 826	Jeffamine D230	NGDE
4.7 ml	2.43 ml	1 ml

Mixing begins by opening the bottle and pouring EPON in a 50 ml beaker and then NGDE and Diamine poured to beaker at the same time until no components stay in bottles. Stirring rod was used to scrape the bottles. They were mixed until the initially ‘;blurry’ mixture turns transparent.

Degasing mixture is crucial to getting rid of the bubbles. Degasing at room temperature decreased bubbles, however it couldn’t abolish bubbles. Heating and degasing simultaneously removed all bubbles. Heating temperature should be 10°C

below to cured material glass transition temperature, otherwise curing in the beaker might be observed. Figure 23 shows a stainless steel degass chamber on the hot plate and high quality vacuum pump. A hose connects the pump to the chamber and sucked air from the mixture.

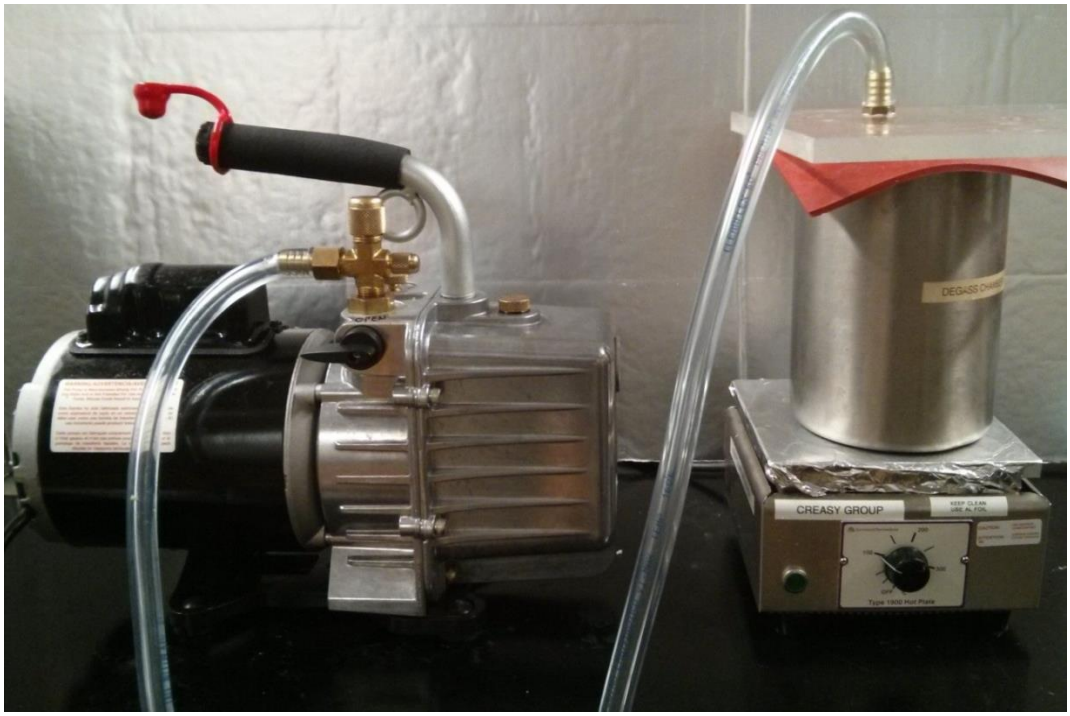

Figure 23. Mixture in beaker was put into the degass chamber that is connected to the vacuum pump.

Pouring can reintroduce bubbles. Preparation started with cleaning the silicone mold with air pressure to remove dust and small particles. During the degassing step, silicone mold sat in a 100 °C oven. Using a hot mold dropped the mixture viscosity all allowed narrow areas to fill easily. From trial and error, the critical place for pouring was found to be the gage section. Best outcome came from filling the gage section and

allowing the resin to flow into the grip region. Once the gage was filled, the ends could be completed by separately pouring the mixture into them.

Finally, the specimens were cured. Constituent's volume ratio is important to obtain targeted material T_g. Obtaining same glass transition temperature is important to collect same material properties. Thus Constituents' volume ratio and curing cycle was taken from Xie. [60] Table 4 presents the curing cycle in detail. Material sat at 130 °C for post curing. Same processing steps applied to tensile and planar tension specimens. Figure 24 shows the planar tension mold inside the oven during curing cycle.

Table 4. Epoxy-based shape memory polymer curing cycle

Heating Temperature	Heating Time
100°C	90 minutes
130°C	60 minutes

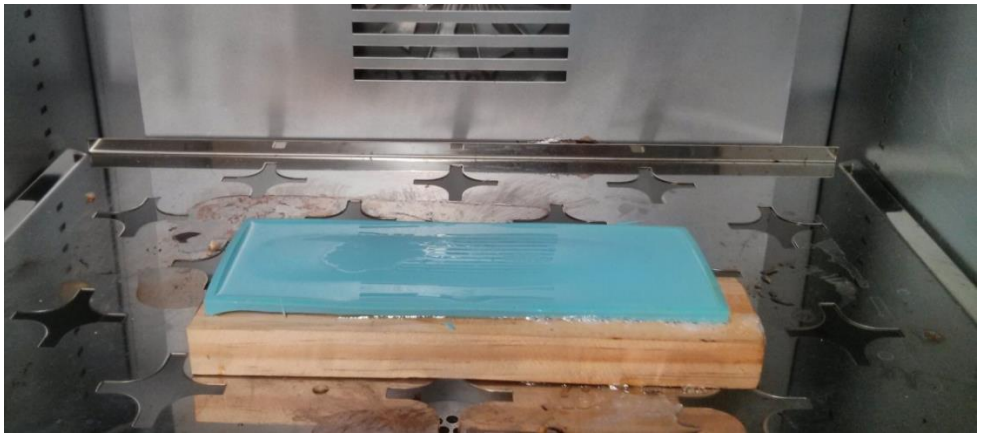

Figure 24. This picture was taken during the planar tension specimen curing process.

4. METHOD

4.1 Thermal Analyses

4.1.1 Differential Scanning Calorimetry (DSC)

Differential scanning calorimetry is a thermal analysis method that measures heat required to increase temperature in a material. Heat flow indicates endothermic and exothermic transitions that characterize the material's glass transition, T_g, or melting point, Tm. A TA Instruments Q20 V24.9 DSC determined the epoxy-based shape memory polymer's glass transition temperature. The DSC machine appears in Figure 25.

Figure 25. Test parameters are arranged by computer. Heat flow provided by right side machine. Nitrogen bottle also include in DSC whole step up.

A DSC specimen is simple: a small continuous mass. It has to fit in a small aluminum pan. The test sample was approximately 2 mm^3, and mass was 0.0108 gram.

Before placing the pan in the machine, an ethyl alcohol wipe removed any fingerprints. Thermal cycle test parameters appear in this list:

DSC Thermal Cycle

1. Equilibrate at 0.00 °C
2. Isothermal for 1.00 min
3. Ramp 10.00 °C/min to 100.00 °C
4. Ramp 10.00 °C/min to 0.00 °C
5. Mark cycle 1 end
6. Ramp 10.00 °C/min to 100.00 °C
7. Ramp 10.00 °C/min to 0.00 °C
8. Mark cycle 2 end

4.2 Tensile Test

Room temperature tensile, high temperature tensile and planar tension tests characterized epoxy-based shape memory polymer's behavior. The experiments used ASTM 638 standards and an instron 4411 test machine produced the tensile data. Bluehill version 2.21 software, which the Instron Company supports, was programmed for obtaining data.

Room temperature tensile test starts with creating test method based on ASTM standards. Test steps and parameters appear in this list:

- Test speed, that is the crosshead speed, was set at 1 mm/min.
- Appropriate grip was assembled to machine
- The operator set the distance between grips was arranged 25.4 mm.
- Material top end was gripped after specimen aligned according to specimen and grip edges
- Material bottom end was gripped See Figure 26 for an illustration

- The test was started to collect the data
- The crosshead moved until the material was broken.
- The test included five specimens.
- Data was collected and analyzed.

Figure 26. Tensile test specimen was positioned between top and bottom grips.

4.2.1 High Temperature Tensile Test

The high temperature tensile test is essential for understanding SMP behavior after transformation. This test is almost the same as the room temperature tensile test except for temperature. The Material is heated twenty or thirty centigrade above T_g to complete the transformation. Heating temperature is vital to obtain 100% rubbery

material. Xie's paper [60] was reviewed to determine final temperature. Dynamic Mechanical Analysis graphs from that paper demonstrate that thirty centigrade above T_g completes the transformation; therefore, that temperature was used with the present specimens.

The oven has a temperature controller to change the internal temperature. A fan inside the oven distributes the hot air by drawing air over the specimen, into a heating chamber, then releasing it at the top and bottom of the oven. The released air flows across the chamber, the moves to the midheight for the oven before it repeats the cycle. The temperature controller and an external thermocouple reader were used to find the specimen temperature. Heating time is crucial to obtain 100% rubbery specimen before started the test. To find a conservative dwell time, a thermocouple was sandwiched between two SMP specimens and placed into the test oven. The specimens were held in the top grip—the bottom grip was open to avoid thermal expansion effects that could put the specimen into tension or compression. The same grips used in the tensile test held these specimens. The oven started to heat to 100 °C. After thirty minutes oven door was opened, the bottom grip was closed on the specimens, and the door was closed again. The oven indicated temperature and the temperature and thermocouple temperature were recorded every minute for four hours. The oven's indicated temperature demonstrated sudden changes while the oven door was open. The outcome was that 30 min heating followed by 40 min reheating was sufficient to produce a specimen that was rubbery throughout its mass.

Previous papers heated specimens for fifteen minutes, which was sufficient to heat the gage section. However, heat distribution should be homogenous throughout the sample to assure that no gradient effects corrupt the test results. Using the experiment noted above, the wait time before a tensile test was set to four hours. High temperature experiments followed this procedure:

- Specimen top end was gripped.
- Oven was started to heat at 100°C.
- Specimen's bottom end was gripped thirty minutes later.
- Room temperature method was applied after waiting four hours to heat
- Four samples were tested to failure.

High temperature cycling test was also performed. Tensile test specimen was used for cycling test. Same heating process was applied for these samples. This test process can be seen below

- Specimen top end gripped.
- Oven started set point 100°C.
- Specimen's bottom end gripped after thirty minutes
- Test applied after waiting four hours from start
- Apply 5% strain to the sample.
- Return top grid to initial position.
- Repeat process applied for four specimens
- Load, extension and cycle count collected.

4.2.2 Planar Tension-Pure Shear Test

Planar tension test is the one method to characterize rubbery material. Although it appears to be a tension test—and it runs in tension—the experiment produces a pure shear state in the specimen because the extension direction stretches, the thickness gets thinner, but gage width is constrained to have no deformation through most of the specimen. The Instron 4411 with a wide serrated grip, which is shown in Figure 27, can perform the planar tension test.

Figure 27. Planar tension one side grips with sharp edges can be seen above.

The planar tension specimen has to be flat and show little surface variation. Planar tension specimen preparation started with checking the sample's waviness. Figure 28 demonstrates surface variation measuring process using a surface plate and micrometer. Grip distance was marked to position specimen accurately. The specimen's gauge

section was marked with small dots so that extension could be tracked optically. HD video was recorded with a Sony Camera during the test.

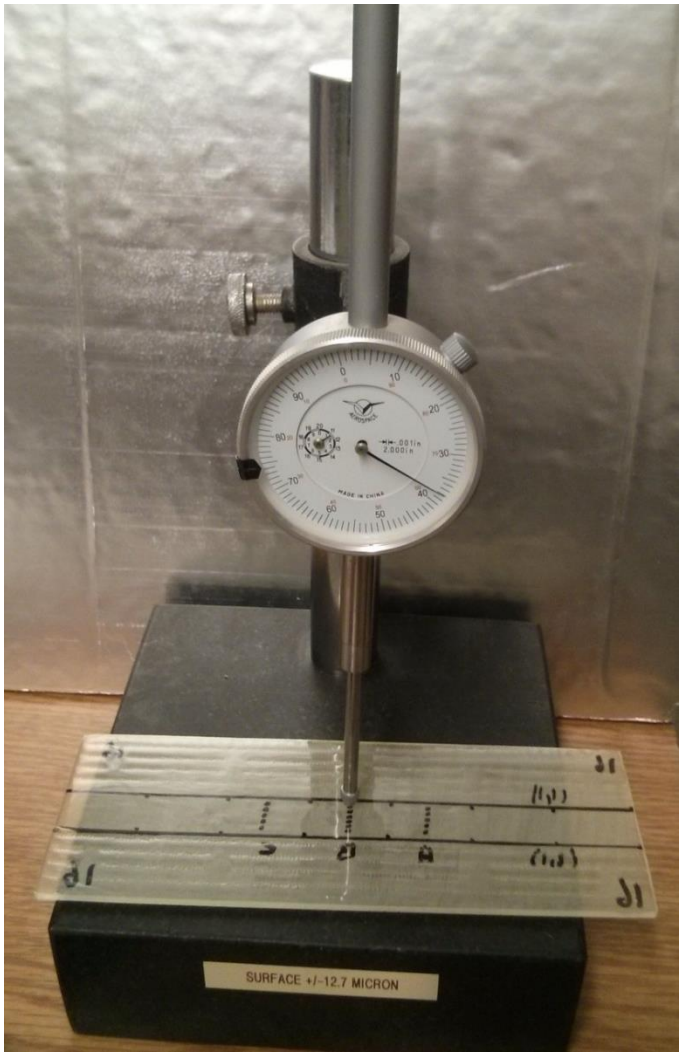

Figure 28. Before running planar tension test, specimen surface variation should be checked.

The pure shear test is for rubbery materials so when applied to SMP it must operate at high temperature. The grip edges were too sharp and caused cracks in the specimens.

Cloth placed between the grip teeth and the specimen softened the effect and allowed good tests. The planar tension experiments followed this procedure:

- Surface variations was checked
- Grip distance was defined by marker.
- Multiple dots were pointed.
- Top and bottom gripped was covered by cloth.
- Specimen top end was gripped. See Figure 29 for an illustration.
- Oven was started to heat at 100°C.
- Sample bottom end was gripped thirty minutes later.
- Camera was started to record after waiting four hours to heat.
- Machine was manually operated to obtain data from software.
- Equal extension was applied to ten times until reach to 5% strain.
- Four samples were tested.

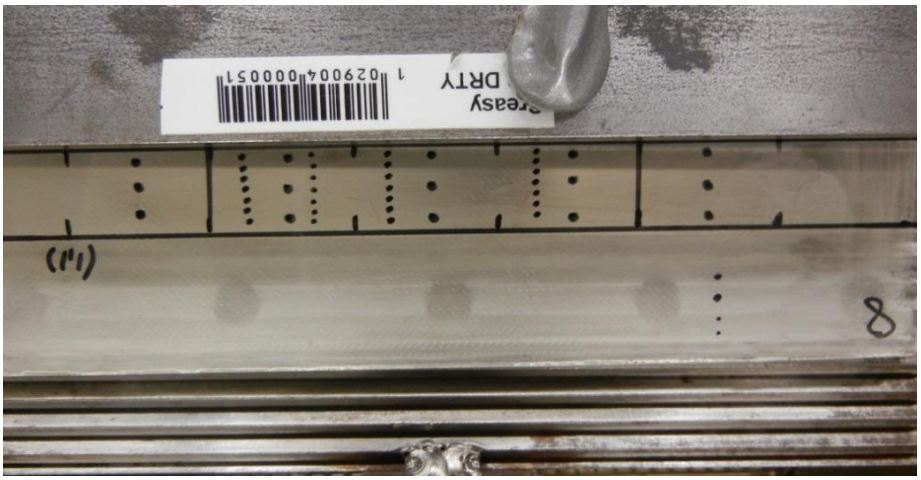

Figure 29: Specimen top side was gripped.

5. RESULTS AND ANALYSIS

This chapter presents fabrication; differential scanning calorimetry results; room temperature and high temperature tensile test results; planar tension test results; and high temperature cyclic test results. No results were possible without fabrication; therefore, the next section covers the fabrication steps.

5.1 Fabrication

Fabrication had two parts: producing the molds, and producing the sample. Producing specimens without critical flaws was a major goal. The same methods were applied while fabricating tensile or planar tensile specimens.

5.1.1 Tensile Specimen

After some initial difficulty with bubbles, specimens like the one in Figure 30 were obtained consistently. The procedure in Chapter 3 is the final procedure used to fabrication the specimens whose data appear in this chapter.

Figure 30.Dog bone tensile specimen made from epoxy-based SMP shows no visible bubbles and other flaws.

5.1.2 Planar Tension Specimen

The Planar tension specimens presented another challenge: obtaining a large, uniform thickness, flat specimen. Specimen flatness was checked by measuring surface variation before performing the test. Initially, the specimens were flat and bubble free; however, after five curing cycles, the silicone mold changed its shape permanently. A dome occurred at the silicone mold's center. This dome formed a curved specimen without equal thickness. Therefore, silicone molds were used for 5 cycles, then discarded.

5.2 Thermal Analysis

Differential Scanning Calorimetry (DSC) using the procedure described in section 4.1.1 found the glass transition temperature for this SMP is 69.9 degree Celsius.

The DSC took the specimen through two thermal cycles to ensure the result was consistent. After putting the aluminum pan into the machine, the DSC cooled the sample to 0 °C. Then the first thermal cycle started and took the specimen 100 °C. The DSC cooled the sample back to 0 Celsius before it repeated the cycle. Figure 31 shows cycle started between -0.5 and -1 heat flow, the sigmoidal blue line around 70 °C shows that a phase change occurred. The software provided the T_g onset point, midpoint and end-point that appear in Table 5.

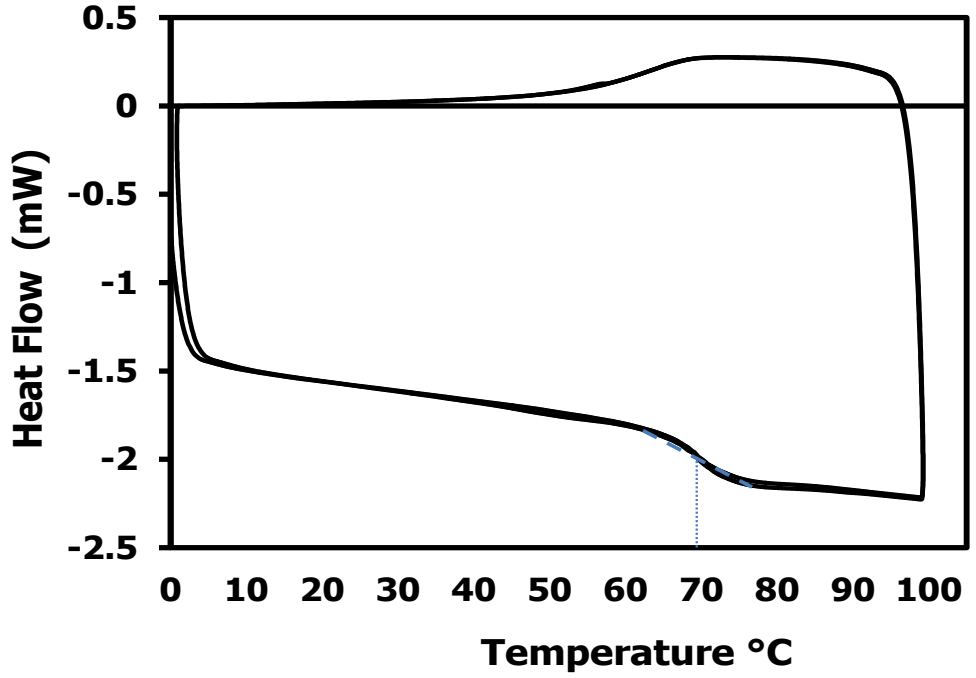

Figure 31. Heat flow vs. Temperature graph obtained from DSC.

Table 5. T_g onset, midpoint, end point values

Onset (°C)	Midpoint (°C)	End (°C)	Height (W/g)	Delta Cp (J/(g·°C)
66.92	69.39	72.32	0.06938	0.4161

5.3 Room Temperature Tension Test

Specimens produced according to ASTM D638 standard were made from epoxy-based SMP. Four specimens were tested to determine ultimate stress and strain properties using these test parameters:

- Crosshead Speed: 1 mm/min
- The Gage length: 7.62 mm
- The Gage cross-section area:≈9.54 mm^2

Software recorded the load (N), extension (mm), data for every 0.1 seconds. Engineering stress is

$$\sigma_e = \frac{F}{A}$$

where σ is stress (MPA), F is force (N) and A is gage cross-section area and engineering strain is

$$\in_e = \frac{\Delta L}{l_o} \times 100$$

where $\in$ is percent strain, ΔL is extension and l_o is gage length in consistent length units. Figure 32 shows four specimens' room temperature tensile stress/strain response. Table 6 presents the maximum stress and strain reached by each specimen.

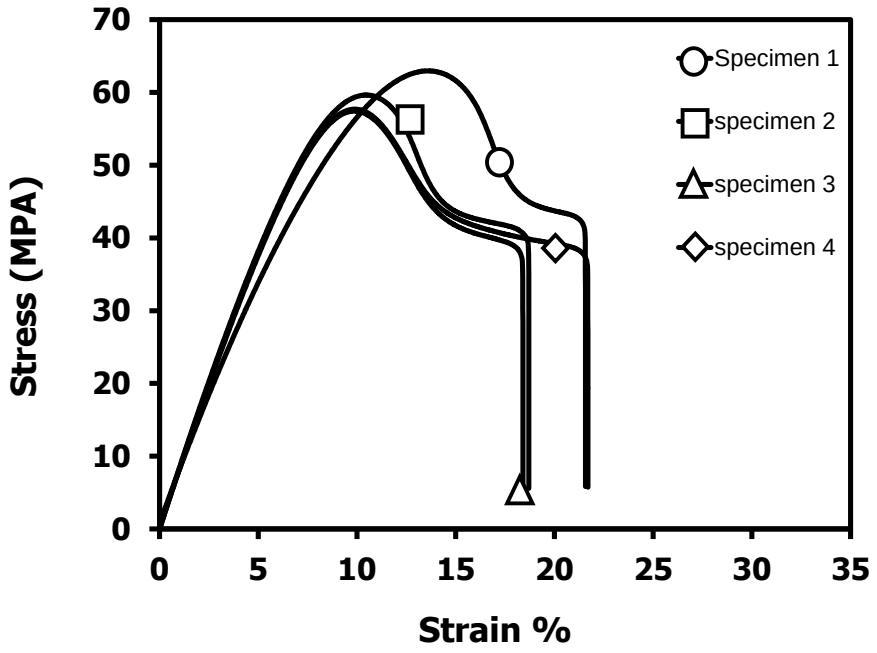

Figure 32. Room temperature tensile test specimen exhibits similar elastic modulus.

Table 6. Room temperature tensile specimen maximum strain and stress values

Specimen	Peak Tensile Stress (MPA)	Failure Strain %
#1	62.96	21.57
#2	57.69	21.69
#3	57.45	18.41
#4	59.64	18.70

5.4 High Temperature Tension Test

The same tensile specimen shape used at room temperature was used at high temperature with the same test parameters.

The first experiments found the time needed to heat these tensile specimens so that they were fully equilibrated at 100 Celsius, which is 30 degrees above the glass transition range. This assures that the specimen is 100 % rubbery during the experiment. This brief experiment found a conservative time for heat to conduct through the material. In Figure 33, an upper line shows the oven temperature and the lower line presents the thermocouple temperature. After 30 minutes heating, the oven door was opened to allow someone to tighten the lower grip. The indicated oven temperature decreased substantially during this process; however, specimen temperature (the lower line marked at circle) exhibited small changes. This makes sense—the oven thermocouple is in the air steam, which immediately gets room temperature air once the door opens. Meanwhile, the specimen thermocouple is sandwiched between two specimens that insulate it from the airstream. The seal is not perfect and some airflow causes the thermocouple to drop faster than the internal material temperature. Although this

experiment shows that the specimens could be fully equilibrated in 90 minutes, this work held the specimens at temperature for four hours before starting an experiment.

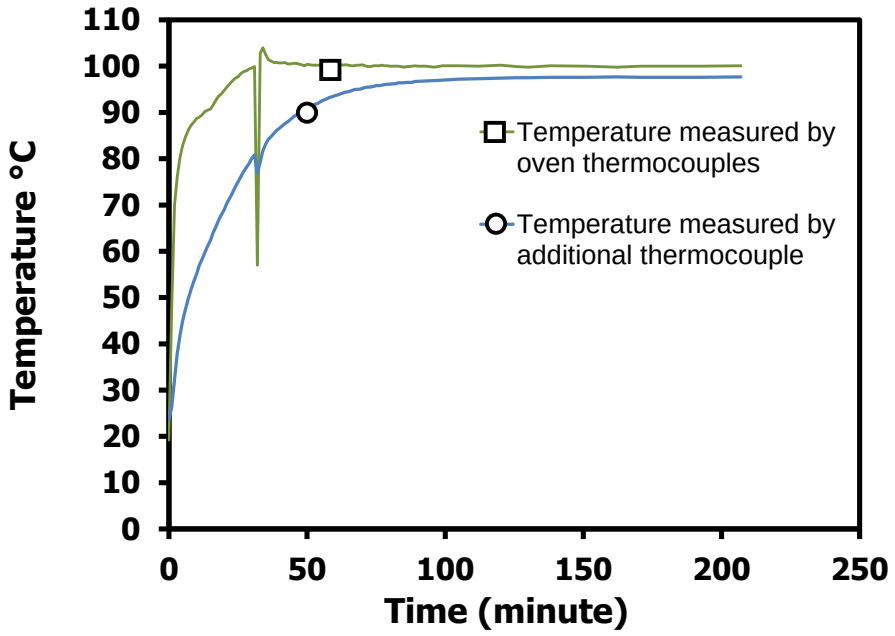

Figure 33. During the heating rate experiment, the oven air temperature and specimen temperature show the lag in heating at the specimen. Because two specimens were sandwiched with a thermocouple between them, the temperature curve shows that 90 minutes is more than sufficient time to complete heat a single specimen to the test temperature.

At high temperature the tensile test was run until the specimens failed. Stress and strain values were found by using same equations mentioned previously. Figure 34 displays specimen stress/strain response, which is slightly nonlinear. When compared to room temperature response, as expected the tensile stress decreased and the strain to failure increased; however, specimens exhibit 50 % strain. Table 7 shows each specimen maximum stress and strain value at high temperature.

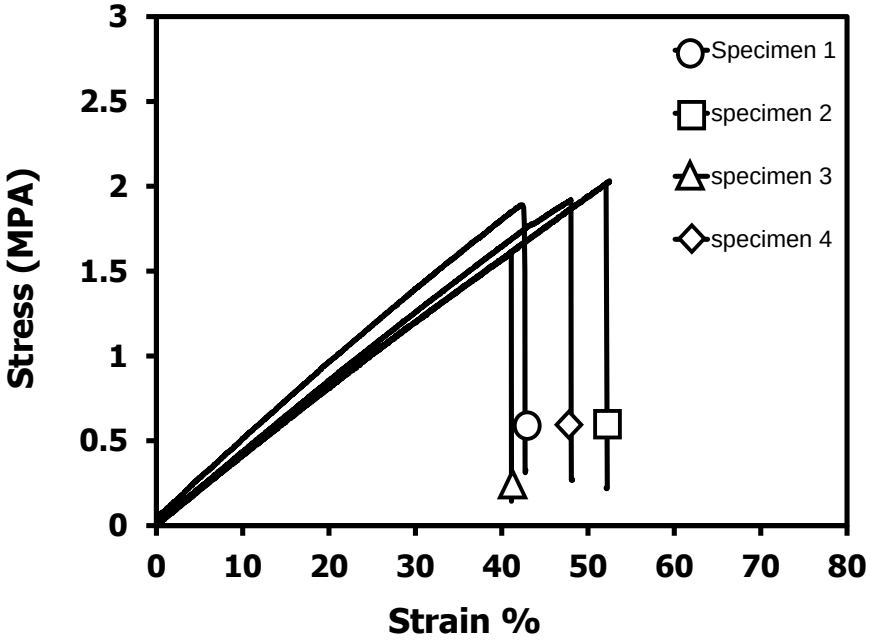

Figure 34. High temperature tensile test performed until to failure.

Table 7. Specimen maximum stress and strain values at high temperature

Specimen	Tensile stress (MPa)	Strain %
#1	1.60	41.14
#2	1.92	48.21
#3	1.88	42.80
#4	2.03	52.49

High temperature true stress/strain values were used for Solidworks nonlinear elastic model analysis. Engineering stress/strain values converted to true stress/strain values by using formulas below.

True stress is

$$\sigma_t = \sigma_e \times (1 + \epsilon_e)$$

True strain is

$$\epsilon_t = \ln(1 + \epsilon_e)$$

Figure 35 presents the room temperature and high temperature tensile responses on single chart. In glass state below glass transition temperature specimens exhibits failure stress two orders of magnitude than rubbery state specimen. In rubbery state specimen shows two times more elongation then glassy state.

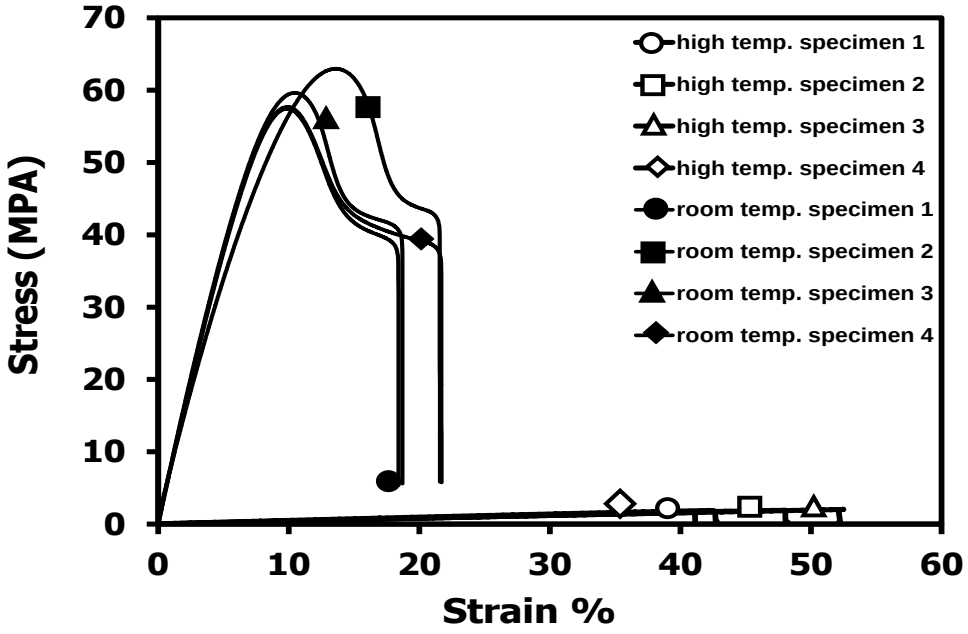

Figure 35. Glassy and rubbery state shape memory polymer response

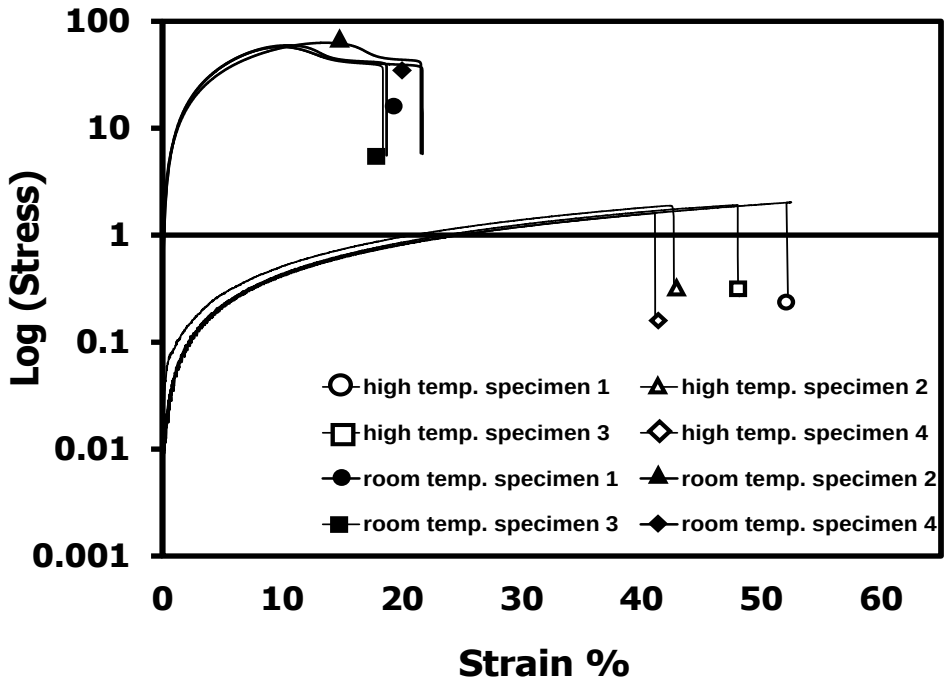

Figure 36. Log scale stress-strain table clearly shows that room temperature stress values are 100 times order of magnitude bigger than high temperature stress values.

5.5 Cyclic Tensile Test

5.5.1 High Temperature Fatigue Test

At this point, we know little about the cyclic lifetime available in epoxy-based SMP; therefore, limited cyclic experiments were performed to assure that the material was characterized so that it provides at a minimum tens or hundreds of cycles without failing. A high temperature fatigue test was run to estimate safe strain range.

Two specimens were used under different strain. First, 52 percent strain was applied to tensile test specimen and during the 3rd cycle, the sample failed. Figure 37 shows the 52% strain specimen and its failure during the 3 cycle. It shows the

specimen cycled to 5.2 percent strain; this specimen run for 192 cycles without breaking. The experiment was stopped arbitrarily because the specimen was healthy and the ultimate performance of the specimen was not within the objective.

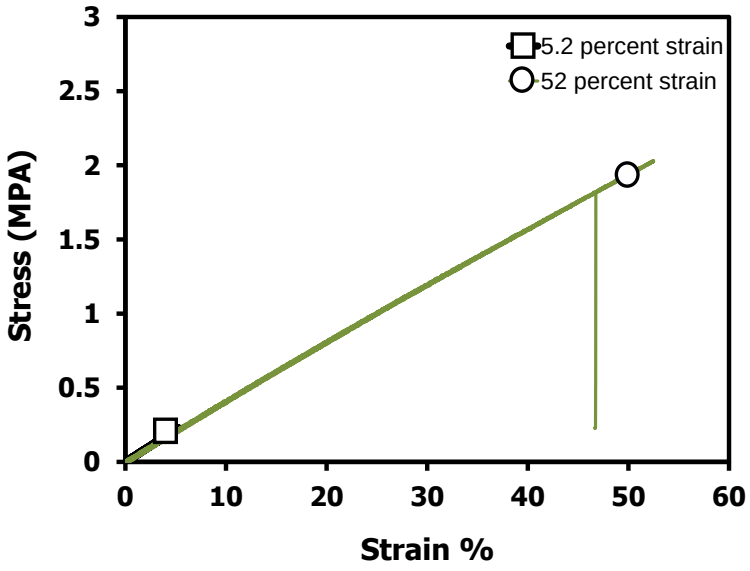

Figure 37. 2 specimens were used for high temperature fatigue test.

5.5.2 High Temperature Cyclic Tensile Test

High Temperature Cycle test was also performed. These test parameters was explained in 4.2.1. 5 % strain were applied each specimen and load, extension was observed. Load and extension were converted to stress and strain respectively. 3 specimens were used for cyclic test. Figure 38 displays stress values when 5.2 % strain apply to specimens. This test was run to confirm Rousseau [62] paper thermomechanical cyclic results.

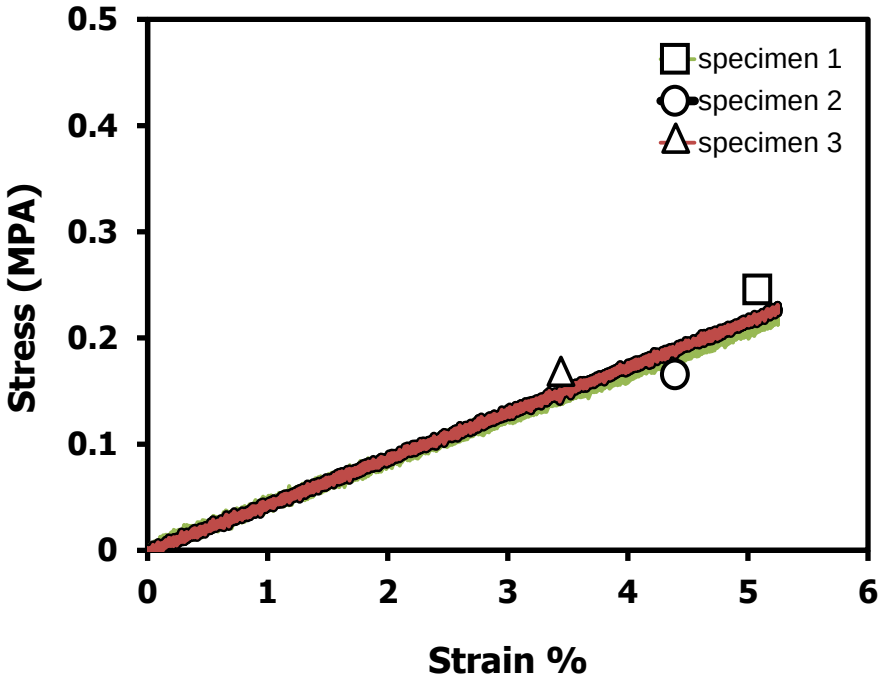

Figure 38. High temperature cyclic test

5.6 Planar Tension-Pure Shear Test

Planar tension test specimens are built from epoxy-based SMP. Cloths were used to avoid unexpected cracks before or during the test. 0.5 % strain applied ten times and each extension was recorded by HD camera to examine exact strain. After applied 5 % strain, video was analyzed by capturing each extensions photo. Each photo was compared to the reference photo that was taken before the any extension was applied. Dots that are in the middle of the specimen were used to realize pixel differences. Figure 39 shows dots that were analyzed for obtaining strain. Matlab image correlation code was used to find original extension. Approximately 2.5 times less strain obtained after analyzing data by Matlab digital image correlation. Results were confirmed by Microsoft paint. Pure shear test parameters can be seen below.

- Gage length: 15 mm
- Specimen aspect ratio: 11.8:1
- 5 % Strain were applied.

Figure 39. Black dots are marked to calculate strain for planar tension test.

Because planar tension test specimens are flat surface variation was controlled by table micrometer. Each specimen measured by eight different points. Average thickness and surface variations was calculated to control the surface waviness. Table 8 shows each point's thickness, average thickness and surface variations.

Table 8. Specimen thickness was measured in eight different points.

sample 8	sample 10	sample 11	sample 14	sample 15
1.13	1.345	0.94	1.4	1.24
1.13	1.33	0.89	1.43	1.23
1.15	1.27	0.88	1.4	1.27
1.18	1.26	0.93	1.43	1.24
1.13	1.32	0.92	1.44	1.22
1.11	1.31	0.89	1.43	1.22
1.14	1.29	0.89	1.4	1.26
1.18	1.24	0.94	1.43	1.2
Standard Deviation				
0.023419	0.034409	0.023452	0.015811	0.021213
Average Thickness				
1.14	1.29	0.91	1.42	1.23
Variation %				
2.047	2.655	2.577	1.113	1.717

Planar tension test load extension appears in Figure 40. Four specimens provided load and extension data. The extension values are too small much smaller than the strain found in the high temperature tensile results.

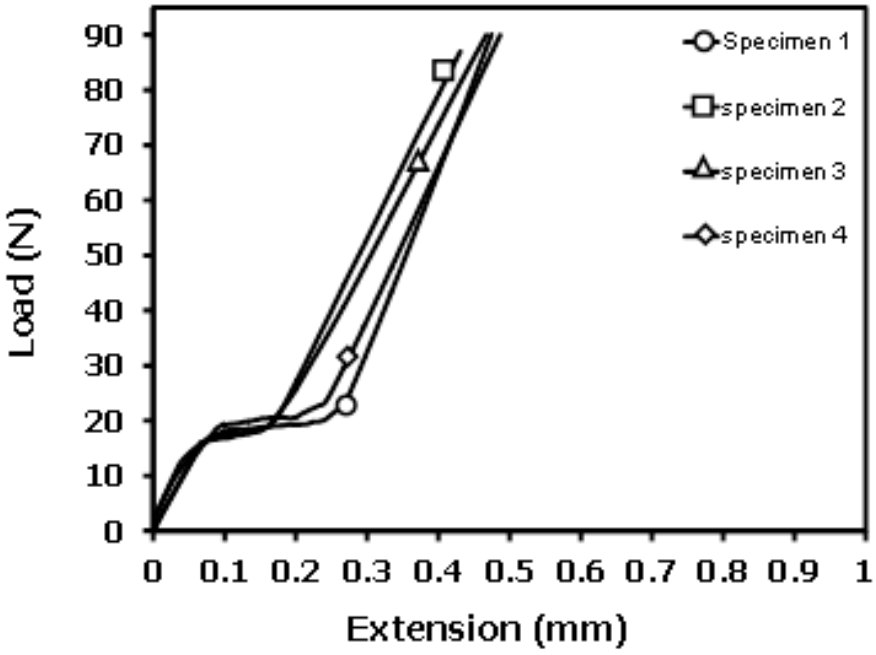

Figure 40. Planar tension test result

At this point, the simple tension results reach strains of 40 % and the planar tension results only obtain 1.4 % strain. If the strain range for both experiments is not approximately the same, the solver in Solidworks cannot find the Ogden model parameters needed to model the material as a hyperelastic material.

According to the literature, the planar tension specimen aspect ratio should not be less than 10:1 in order to keep the specimen edge effects small. Our specimen aspect ratio was greater, 11.8:1, to obtain better results; however, compared to the simple tension result, the strain to failure was small. This was a surprising outcome.

Therefore, the planar tension test was repeated with a specimen with a 10:1 aspect ratio. This work will call the 11.8:1 aspect ratio experiment wide PT and the 10:1 aspect ratio specimen narrow PT. Figure 41 shows narrow and wide PT results with

specimens run to failure. Narrow PT reaches higher stress and strain than the wide PT. The opposite would be true for typical elastomers. This outcome requires further discussion and analysis.

Conventional elastomers are compliant and have a low, but critical crosslink density that enables their unique mechanical properties. Epoxy-based SMPs have higher crosslink density, but show elastomeric behavior under more limited stretch. The planar tension results should show a higher stress at any stretch or strain level than the stress obtained by simple tension. Because the planar tension adds width, the transverse deformation is restricted, which increased the load needed to strain the material. The outcome from wide PT and narrow PT specimens suggest that, given the greater crosslink density of epoxy SMP, a typical 10:1 specimen might be over constrained. Future experiments with the material should look at specimens narrower than 10:1 and determine the limit on width needed to obtain at least 50% of the stretch obtained from the simple tension test. Then, the data set strain ranges would be balanced and the right material model (hyperelastic, etc.) could be found. The narrower specimen will have significant edge effect load. Removing the edge effect load would require either running two specimens and subtracting their load/displacement curves, or using finite element analysis to study the deformation field and extract the correct load/displacement data from the pure shear region.

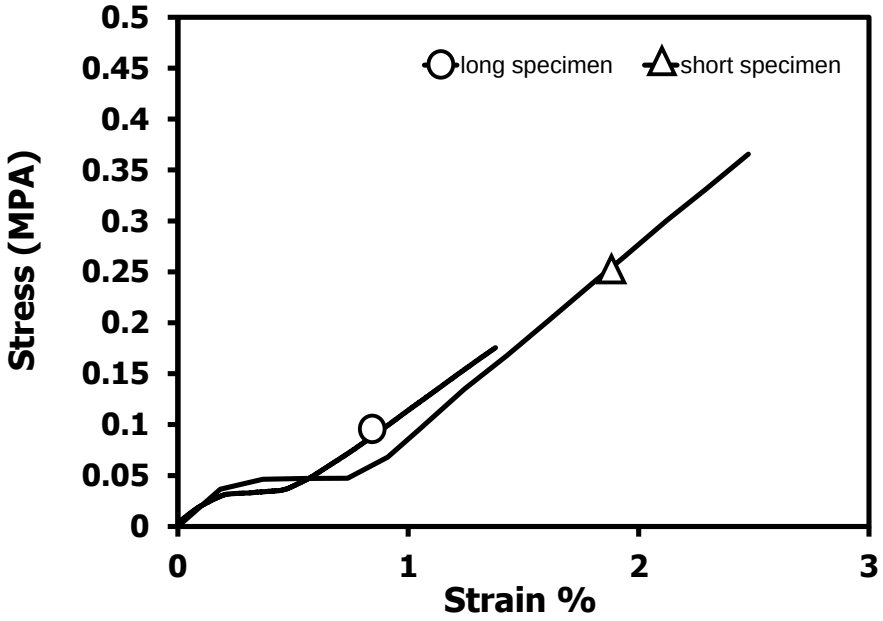

Figure 41. Long specimen that has 11.8 aspect ratio exhibited less stress and less strain.

6. APPLICATION TO DESIGN AND NUMERICAL ANALYSIS

6.1 Objective

Hyperelastic material models require properties derived from three experiments: simple tension, planar tension, and biaxial tension. [72, 73] The objective is to take the experimental properties and find a suitable hyperelastic material model for numerical analysis.

6.2 Analysis

The first question is whether a hyperelastic model is necessary. As a baseline, it is best to start with the minimal possible model and then determine if a higher level model must be used. Therefore, the first model applied to the problem is a nonlinear elastic, isotropic material. The nonlinear elastic isotropic material uses the high-temperature true stress strain curve as its foundation. For this analysis, the nonlinear elastic model will use the simple tension result and attempt to predict the performance obtained in the simple tension and planar tension experiments. If both tension behaviors appear in the finite element outcome, it means that, although rubbery, epoxy SMPs do not exhibit hyperelastic behavior. However, if simple tension can be modeled while planar tension cannot, it means that the SMP is showing some hyperelastic response. Finally, if the simple tension experiment cannot be modeled from the simple tension data alone, it means that the SMP shows significant hyperelastic response—typical elastomer simple tension behavior cannot be modeled from simple tension experiments as the only data because the three dimensional response is too complex

6.2.1 Predicted Shape Change in Simple and Planar Tension

The simple tension specimen's gage section was analyzed in Solidworks using the simple tension experimental results listed in Table 9. Fixing the specimen is important. If specimen is under constrained, it will move in virtual space and the model will accelerate without converging on a solution. If over constrained, the model will be stiffer than the experiment and the response will not match the experiment. The finite element models used for simple and planar tension is the specimen's gage section alone—using only the key portion for the model saves time in analysis. First, the bottom surface, which has Y as its surface normal, was prohibited from moving in Y. This—when combined with a force or displacement applied to the distant, Y-normal face, will cause the model gage length to stretch. However, the model is not stable. Small round-off errors will generate some net force in the X and Z directions. The boundary conditions must inhibit this motion while keeping the cross section free to contract under Poisson's ratio effects. Therefore, a second boundary condition restricted the bottom, Y-normal face. This condition prohibited the edge parallel with the X axis from moving in Z.

By limited this edge in Z, the edge is free to contract by Poisson effects and the model is almost stable. At this point, the model cannot move in Z or Y, but the X direction is free. Finally the model is locked from free body motion by choosing one vertex along the edge that was restricted in Z and fixing that point in all three directions. The software warned that the model was not absolutely fixed in space; however, this was not a problem. The software adds a small adjustment to stabilize the model. With the

bottom side fixed, displacement equivalent to 40% strain—the same strain value obtained from experiment—was applied at the gage section's top end. Figure 42 shows the gage section boundary conditions. Figure 43 shows the fixed point on the restricted edge.

Table 9. These true stress/true strain data were uploaded into Solidworks for nonlinear elastic analysis.

True Strain	True Stress (MPa)
0.02464	0.1169
0.04885	0.2239
0.07294	0.3366
0.09647	0.4432
0.1194	0.5559
0.1418	0.6694
0.16385	0.7778
0.1853	0.8912
0.2063	0.9991
0.2269	1.103
0.2471	1.213
0.2669	1.322
0.2863	1.4323
0.3054	1.533
0.3240	1.640
0.342	1.750
0.3604	1.852
0.3781	1.943

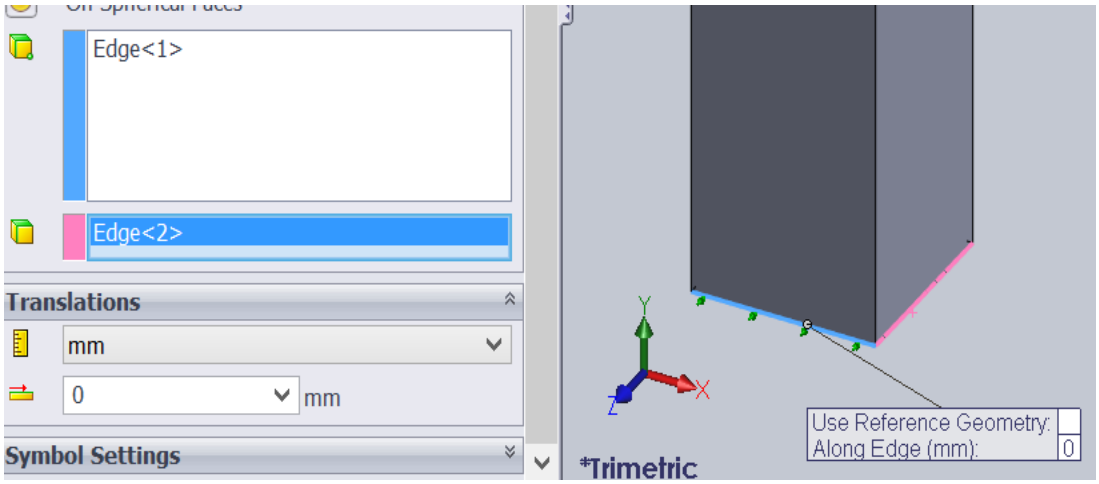

Figure 42. Constraining one of the edges parallel with X will not over constrain the model if that edge cannot move in Z and if no other edges are constrained. Here, the edge parallel to X is fixed using the edge parallel to Z as the reference direction. Set the motion to zero.

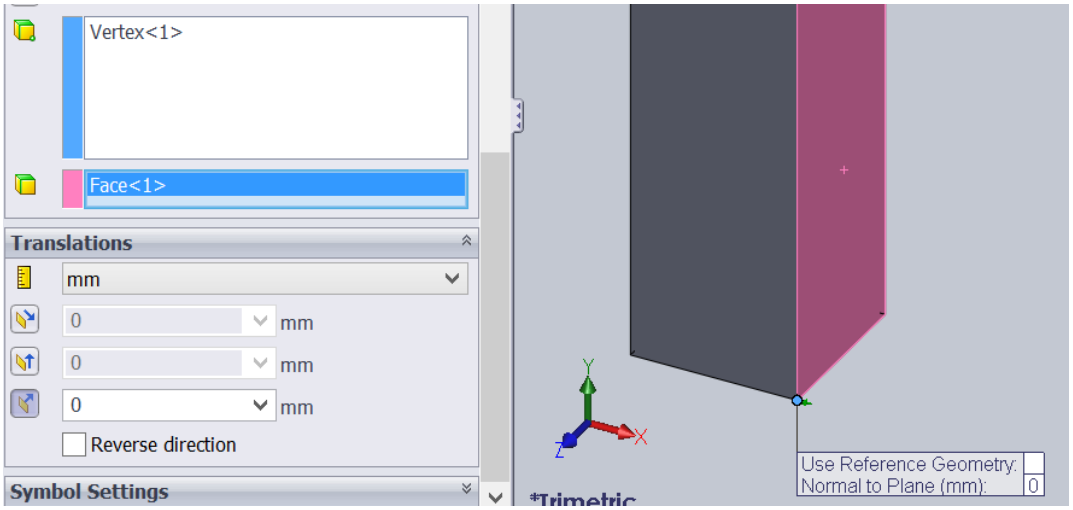

Figure 43. The point (vertex) picked here cannot move in X because we selected the face with a normal in the X direction as the reference and set motion in the normal direction to zero mm.

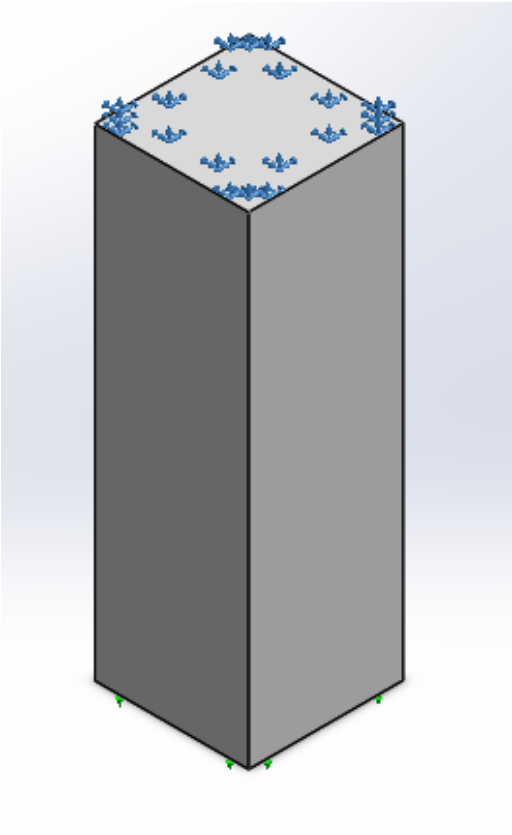

Figure 44. Blue arrows shows displacement direction and green arrows at the bottom shows fixed position for tensile specimen.

Figure 44 shows simple tension gage length, fixing and load applying points. Planar tension specimen also simulated in Solidworks. Same specimen length and thickness dimensions used to design model. However specimen height decreased to gage length. Same fixing method was used for planar tension specimen. Specimen bottom side, bottom edges and vertex fixed and 1.8 % strain is applied to specimen top side. Figure 45 Demonstrates analyzed specimen boundary conditions.

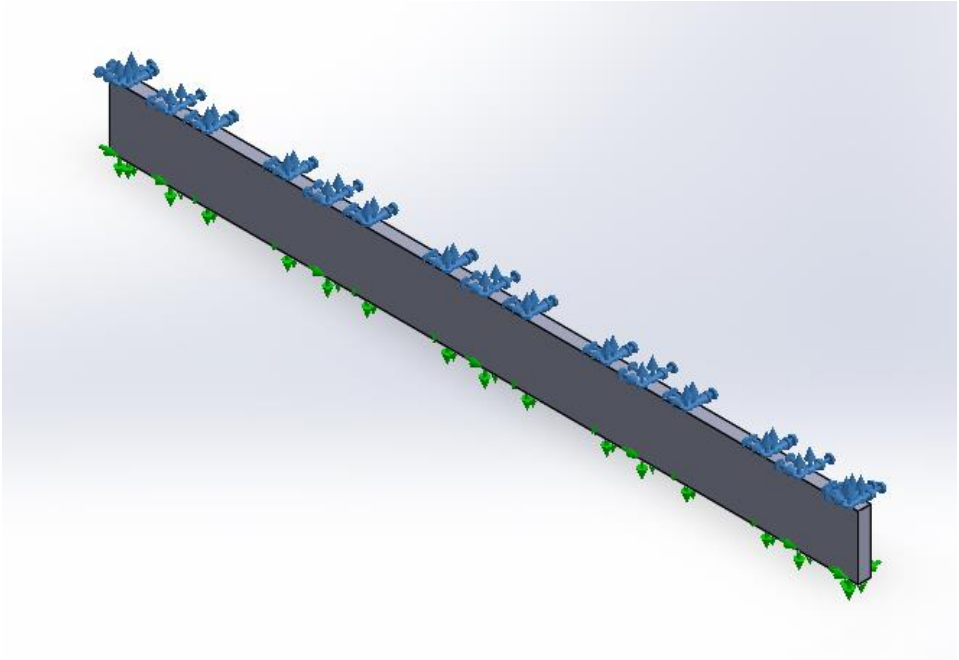

Figure 45.Blue arrows shows displacement direction and green arrows at the bottom shows fixed position for planar tension specimen.

6.3 Results

Results for simple tension with a nonlinear elastic model were compared to experimental results to determine if the nonlinear elastic model describes the performance. Figure 46 shows simple tension experiment data compared to FEA analysis. The data in Table 9 are true stress/true strain. The FEA output is engineering strain; therefore, the stress and strain were converted to true values using the same equations noted above. The FEA model reached 25 % strain and matches the simple tension well. If the nonlinear model is appropriate for this material, is should predict all tensile behaviors in the experiments. The next experiment to model is the planar tension test.

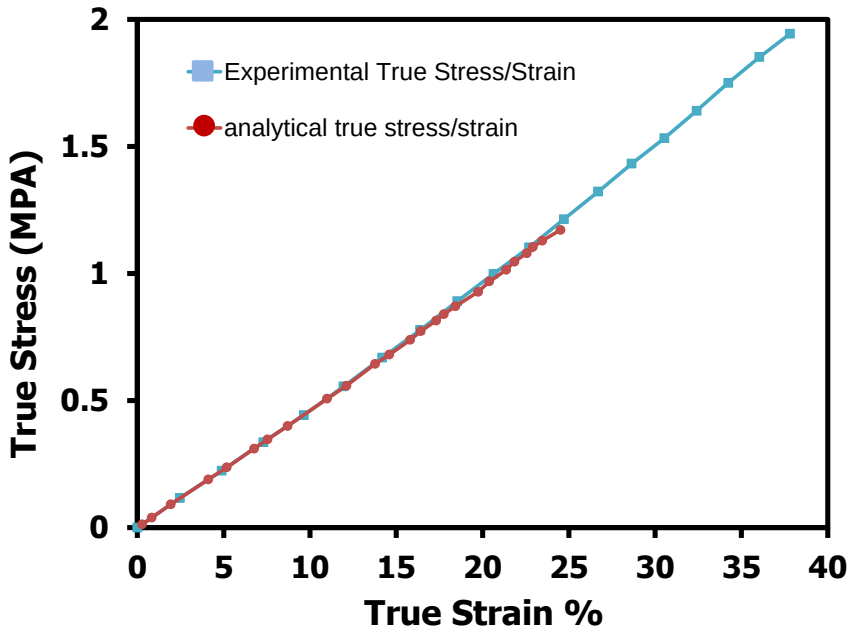

Figure 46. Nonlinear elastic solidworks results and high temperature tensile results are matched until 25 % strain.

The same analysis process applied to planar tension specimen resulted in Figure 47. It is clearly seen that experimental and analytical planar tension behavior are different. The nonlinear material model cannot capture the complex response in planar tension. This is strong evidence that the material is not a simple, nonlinear elastic system. A hyperelastic material model must be applied.

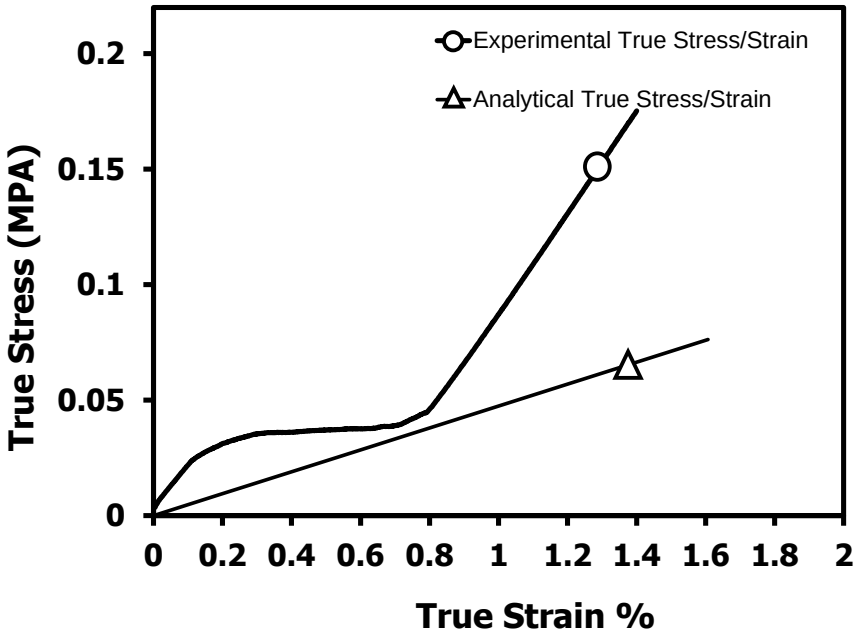

Figure 47. Experimental and solidworks planar tension results show different behavior.

Figure 48 shows the tensile test results with the planar tension results from experiment and analysis. The unexpected outcome is that the planar tension test fails as such small strains. Planar tension should always have greater stress than simple tension because the constraint in transverse deformation adds a stiffening effect to the material. However, the planar tension test is for high strain (high stretch) elastomers. It might be necessary to use new specimen geometry to extract the hyperelastic parameters.

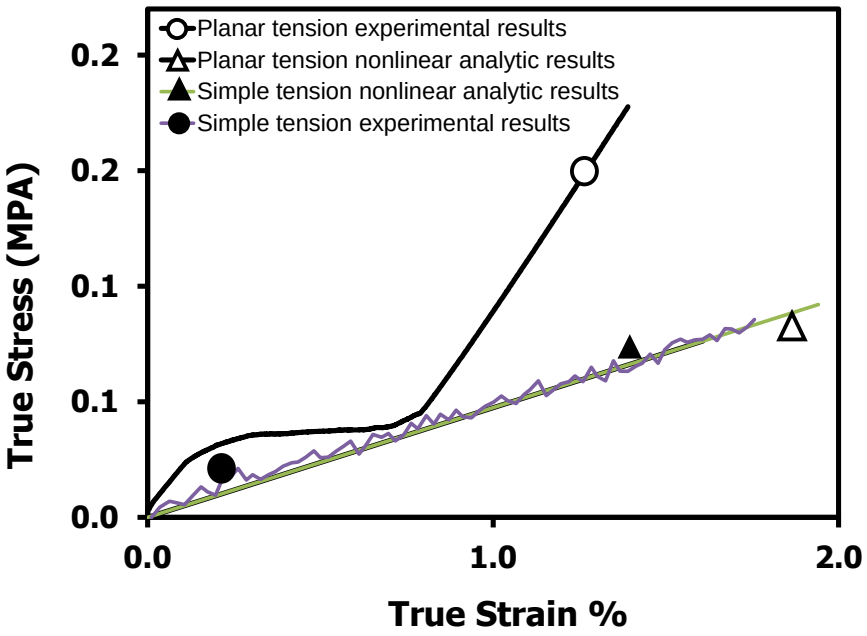

Figure 48.Simple tension stress/strain values are similar analytical planar tension values.

7. FINDINGS AND CONCLUSIONS

Epoxy based SMP was tested to check for hyperelastic behavior and to obtain the hyperelastic constants. Room and high temperature simple tension, high temperature planar tension, cyclic tensile, and fatigue test were run to get initial information about the material's behavior.

There is no hysteresis or Mullins effect observed during tensile and planar tension tests. Although exhibiting elastomeric response—that is, large elastic shape changes—the material does not require conditioning to provide repeatable response in cyclic tests. This is likely caused by the high crosslink density in the material making it stable.

Planar tension results show significant deviation from simple tension results. Thus, the material is not a simple nonlinear elastic system. The standard planar tension experiment was not suited to this highly crosslinked, stretch-limited material. The hyperelastic parameters could not be obtained from the analysis. Therefore, a new test specimen should be developed to extract the properties suggested from the planar tension response.

High temperature test strain values must be analyzed by digital image correlation methods. Strain values from crosshead data were approximately 2.5 times bigger than actual strain values measured using Matlab DIC code.

Tensile specimen analysis matched the experiment when the nonlinear elastic material model was used. However, that model does not predict the behavior found using

the planar tension experiment. This suggests a hyperelastic material model is needed, even for this limited stretch material.

For future work, a new test specimen design is needed to obtain the hyperelastic parameters. Planar tension specimens have a 10:1 width to length ratio in the gage section to make the edge effects small. For epoxy SMP the experiments suggest that the high aspect ratio is extreme because the strain to failure in planar tension is nowhere near that obtained in simple tension. Either this aspect ratio should decrease or a new specimen should be designed. Reducing the aspect ratio will increase the edge effect and some combined experiment/analysis might be needed to address data extraction.

Biaxial tension or lubricated compression experiments should be done to completely define all SMP hyperelastic behavior. Given the restricted stretch in this material, lubricated compression might be enough to collect the data. Some care with the diameter/thickness ratio might be needed.

REFERENCES

[1] Scholz M.S., Blanchfield, J.P., Bloom, L.D., Coburn, B.H., Elkington, M., Fuller, J.D., Gilbert, M.E., Muflahi, S.A., Pernice, M.F., Rae, S.I., 2011, "The Use of Composite Materials in Modern Orthopaedic Medicine and Prosthetic Devices: A Review," *Composite Science and Technol*ogy, **71** (16), pp. 1791–1803.

[2] Fu T, Zhao J-L, Xu K-W., 2007, "The Designable Elastic Dodulus of 3-D Fabric Reinforced Biocomposites," *Material Letters*, **61** (2), pp. 330–333.

[3] Evans SL, Gregson PJ., 1998, "Composite Technology in Load-Bearing Orthopedic Implants," *Biomaterials*, **19** (15), pp. 1329–1342.

[4] Ramakrishna S et al., 2001," Biomedical Applications of Polymer-Composite Materials: a Review," *Composite Science and Technol*ogy, **61** (9), pp. 1189–1224.

[5] Orthotic& Prosthetic Design Inc., "Prosthetics" *Prosthetic Limb with Orthopedic Socket*, Retrieved April 10, 2014 from http://www.oandpdesign.com/prosthetics.htm.

[6] Morrison, B. J., Creasy, T. S., Polliack, A. A. and Fite, R. 2002, "A New Fabrication Technique Utilizing a Composite Material Applied to Orthopedic Bracing," *Polymer Composites*, **23**, pp. 10–20.

[7] J. Hu, 2007, "Shape Memory Polymers and Textiles." *Woodhead Publishing Ltd*.

[8] S. Kelch and A. Lendlien, 2002, "Shape Memory Polymers," *Angewandte Chemie International Edition in English*, **41**, pp. 2034-2057.

[9] K. P. Seward and P. A. Krulevitch, *2002,* "Shape Memory Alloy/Shape Memory Polymer Tools," US *Patent, 142119, A1*.

[10] Maitland, D. J., Metzger, M. F., Schumann, D., Lee, A. and Wilson, T. S. 2002, "Photothermal Properties of Shape Memory Polymer Micro-Actuators for Treating Stroke," *Lasers in Surgery and Medicine*, **30** pp. 1–11.

[11] E. A. Snyder and T. H. Tong, 2005, "Towards Novel Light-Activated Shape Memory Polymer: Thermomechanical Properties of Photo-Responsive Polymers," *Materials Research Society Symposium Proceedings*, San Francisco, CA.

[12] H. J. Yoo, Y. C. Jung, N. G. Sahoo and J. W. Cho, J., 2006, "Polyurethane Carbon Nanotube Nanocomposites Prepared by in-situ Polymerization with Electro Active Shape Memory," *Journal of Macromolecular Science: Physics*, **45** (4), pp. 441-451.

[13] H. Adachi, T. Yokoi, T. Hatori, K. Morishita, K. Sakashita, H. Kaiya, K. Inoue, Y. Ueda, T. Nakamura and S. Yamaguchi, 1990, "Temperature Display Devices," *Japan Patent, 02124438*.

[14] K. Kobayashi and S. Hayashi, 1990, "Acoustic Sensors Using Polymers with Shape Memory," *Japan Patent, 02183132*.

[15] S. Kondo and S. Hayashi, 1991, "Shape Memory Polymer for Use as Sensor in Frozen Preservation," *Japan Patent, 03183920*.

[16] Y. Osada, 1995, "Heat-Sensitive Reversible Shape-memory Hydrogels," *Japan Patent, 07292040*.

[17] Lendlein Andreas, and Robert Langer, 2002, "Biodegradable, Elastic Shape-Memory Polymers for Potential Biomedical Applications," *Science,* **296** (5573), pp. 1673-1676.

[18] R. S. Langer and A. Lendlein, 2003, "Biodegradable Shape Memory Polymeric Sutures," *World Patent, WO 088818 A2*.

[19] H. M. T. Wache, D. J. Hentrich and M. H. J Wagner, J., 2003, "Development of a Polymer Stent with Shape Memory Effect as a Drug Delivery System," *Journal of Material Science: Materials in Medicine*, **14** (2), pp. 109-112.

[20] Gall Ken, et al., 2005, "Thermomechanics of the Shape Memory Effect in Polymers for Biomedical Applications," *Journal of Biomedical Materials Research Part A,* **73** (3) pp. 339-348.

[21] Sokolowski, Witold, et al., 2007, "Medical Applications of Shape Memory Polymers," *Biomedical Materials,* **2** (1), pp. 23-27.

[22] Lendlein A., Behl M., Hiebl B., Wischke C., 2010, "Shape-Memory Polymers as a Technology Platform for Biomedical Applications," *Expert Review of Medical Devices,* **7** (3), pp. 357-379.

[23] Metcalfe A, Desfaits AC, Salazkin I, Yahia L, Sokolowski WM, Raymond J, 2003, "Cold Hibernated Elastic Memory Foams for Endovascular Interventions," *Biomaterials*, **24** (9), pp. 491-497.

[24] Yakacki CM, Shandas R, Lanning C, Rech B, Eckstein A, Gall K., 2007, "Unconstrained Recovery Characterization of Shape-Memory Polymer Networks for Cardiovascular Applications," *Biomaterials*, **28** (14), pp. 2255–2263.

[25] Everhart MC, Stahl J, 2005, "High Strain Fiber Reinforced Reusable Shape Memory Polymer Mandrels," *International SAMPE Symposium and Exhibition*, Long Beach, CA.

[26] Arzberger SC, Munshi NA, Lake MS, Barrett R, Tupper ML, Keller PN, Francis W Campbell D, Gall K, 2004, "Elastic Memory Composites for Deployable Space Structures," *National Space Missile and Materials Symposium,* Seattle, WA.

[27] Lake MS, Hazelton CS, Murphey TW, Murphy D, 2002, "Development Of Coilable Longerons Using Elastic Memory Composite Material," *Structures, Structural Dynamics, and Materials Conference*, Reston, VA.

[28] Campbell D, Lake MS, Scherbarth MR, Nelson E, Six RW, 2005*," E*lastic Memory Composite Material: An Enabling Technology for Future Furlable Space Structures," *Structures, Structural Dynamics, and Materials Conference*, Reston, VA.

[29] Vaia R, Baur J, 2008, "Adaptive composites," *Science*, **319**, pp. 420.

[30] Spintech Inc., "Smart Mandrels," *Reusable Mandrel for Filament Winding*, Retrieved March 30, 2014 from http://www.smart-tooling.com/investigate-mandrels.html

[31] Cornerstone Research Group Inc., "Morphing Systems," *Morphing Wings*, Retrieved April 5, 2014 from http://www.crgrp.com/rd-center/morphing-systems

[32] Hu J, Ding X, Tao X, Yu J,2002, "Shape Memory Polymers and Their Applications to Smart Textile Products," *Journal of Donghua University (English Edition)*, **19**, pp. 89.

[33] Mondal S, Hu JL, 2006, "Temperature Stimulating Shape Memory Polyurethane for Smart Clothing," *Indian Journal of Fibre and Textile Research*, **31**, pp. 66.

[34] M. Behl, J. Zotzmann, and A. Lendlein, 2010, "Shape-Memory Polymers and Shape Changing Polymers," *Advances in Polymer Science*, **226**, pp. 1-40.

[35] Scarborough Stephen E. and David P. Cadogan, 2006, "Applications of Inflatable Rigidizable Structures," *International SAMPE Symposium and Exhibition (Proceedings)*, Long Beach, CA.

[36] Mayo Foundation for Medical Education and Research, 2010, "Minimally invasive surgery," Retrieved April 3, 2014 from http://www.mayoclinic.org/tests-procedures/minimally-invasive-surgery/basics/definition/prc-20025473

[37] Frost & Sullivan, 2008, *"Medical Device Technologies Changing Healthcare"* N39F-54: 20, TX.

[38] Hodgson N. C. F., Malthaner R. A., Ostbye T., 2000. "The Search for an Ideal Method of Abdominal Fascial Closure – a Meta-Analysis," *Annals of Surgery*, **231** (3), pp. 436–442.

[39] Bai, Y., Jiang, C., Wang, Q., & Wang, T., 2013, "A Novel High Mechanical Strength Shape Memory Polymer Based on Ethyl Cellulose and Polycaprolactone," *Carbohydrate Polymers*, **96** (2), pp. 522-527.

[40] Grosh, P., 2012, "Model Development and Simulation of the Response of Shape Memory Polymer," Phd Thesis, Texas A&M University, College Station, TX.

[41] T. Okano, 1993, "Molecular Design of Temperature-Responsive Polymers as Intelligent Materials," *Advances in Polymer Science*, **110**, pp. 179-197.

[42] Gil Eun Seok and Samuel M. Hudson, 2004, "Stimuli-Reponsive Polymers and Their Bioconjugates," *Progress in Polymer Science*, **29** (12) pp. 1173-1222.

[43] Anis A., Faiz S., Luqman M., Poulose A.M., Gulrez S.K.H., Shaikh H., Al-Zahrani S.M., 2013, "Developments in Shape Memory Polymeric Materials," *Polymer-Plastics Technology and Engineering*, **52** (15) pp. 1574-1589.

.

[44] Wei, Z. G., R. Sandstroröm, and S. Miyazaki, 1998, "Shape-Memory Materials and Hybrid Composites for Smart Systems: Part I Shape-Memory Materials," *Journal of Materials Science*, **33** (15), pp. 3743-3762.

[45] J. M. G. Cowie, 1997, "Chemie und Physik der Synthetischen Polymeren, Vieweg, Braunschweig," pp. 278- 405; J. M. G. Cowie, 1991, "Polymers: Chemistry and Physics of Modern Materials 2nd ed.," *Chapman & -Hall.*

[46] J. Falbe, M. Regitz, 1998, "Rˆmpp lexikon chemie," *Thieme*, **4** (10), p. 2586.

[47] Hu J L, Meng Q H, Zhu Y, Lu J and Zhuo H T., 2007, "Shape Memory Polymers Prepared by Wet, Reaction, Dry, and Electro spinning," *US Patent 11907012.*

[48] Lendlein A and Langer R. S., 2004, "Self-Expanding Device for the Gastrointestinal or Urogenital Area," *US Patent 004776.*

[49] Marco D and Eckhouse S., 2007 "Bioerodible Self-Deployable Intragastric Implants," *US Patent 0156248.*

[50] Behl M and Lendlein A., 2010, "Triple-Shape Polymers," *Journal of Material Chemistry,* **20**, pp. 3335–3345.

[51] Li J, Liu T, Xia S, Pan Y, Zheng Z, Ding X and Peng X, 2011, "A Versatile Approach to Achieve Quintuble-Shape Memory Effect by Semi-Interpenetrating Polymer Networks Containing Broadened Glass Transition and Crystalline Segments," *Journal of Material Chemistry,* **21**, pp. 12213–12217.

[52] Fulcher J. T., Karaca H. E., Tandon G. P. and Lu Y. C., 2013, "Thermomechanical and Shape Memory Properties of Thermosetting Shape Memory Polymer Under Compressive Loadings," *Journal of Applied Polymer Science*, **129,** pp. 1096–1103.

[53] Wei K., Zhu G., Tang Y., Tian G., Xie J., 2012, "Thermomechanical Properties of Shape-Memory Hydro-Epoxy Resin," *Smart Materials and Structures,* **21** (5), 055022.

[54] P. T. Mater, B. S. Kim, Q. Ge, C. Liu, 2004, "Synthesis of Non-ionic Telechelic Polymers Incorporating POSS and Uses Thereof," *US patent, 024098.*

[55] P. T. Mather, B. S. Kim, Q. Ge, C. Liu, 2004, "Preparation and Uses of Non-ionic Telechelic Polymers Incorporating POSS," *World patent, 011525.*

[56] G. Rabani, H. Luftmann, A. Kraft Polymer, 2006, "Synthesis and Characterization of Two Shape-Memory Polymers Containing Short Aramid Hard Segments and Poly(ε{lunate}-Caprolactone) Soft Segments," *Polymer*, **47** (12), pp. 4251–4260.

[57] F. Li, Y. Chen, W. Zhu, X. Zhang, M. Xu Polymer, 1998, "Shape Memory Effect of Polyethylene/Nylon 6 Graft Copolymers," *Polymer*, **39**, pp. 6929–6934.

[58] Kim B.K., Shin Y.J., Cho S.M., Jeong H.M., 2000, "Shape Memory Behavior of Segmented Polyurethanes with an Amorphous Reversible Phase: The Effect of Block Length and Content," *Journal of Polymer Science Part B: Polymer Physics,* **38** (20), pp. 2652-2657.

[59] Atli B, Gandhi F, and Karst G, 2009, "Thermomechanical Characterization of Shape Memory Polymers," *Journal of Intelligent Material Systems and Structures,* **20**, pp. 87–95.

[60] Xie T and Rousseau I A, 2009, “Facile Tailoring of Thermal Transition Temperature of Epoxy Shape Memory Polymers,” *Polymer*, **50**, pp. 1852–1856.

[61] Rimdusit S., Lohwerathama M., Hemvichian K., Kasemsiri P., Dueramae, 2013, “Shape Memory Polymers from Benzoxazine-Modified Epoxy,” *Smart Material Structure,* **22** (7), 075033.

[62] Rousseau Ingrid A., and Tao Xie., 2010, "Shape Memory Epoxy: Composition, Structure, Properties and Shape Memory Performances," *Journal of Materials Chemistry*, **20** (17), pp. 3431-3441.

[63] Xie T., Xiao X., and Cheng Y., 2009, “Revealing Triple-Shape Memory Effect by Polymer Bilayers,” *Macromolecular Rapid Communication,* **30**, pp. 1823–1827.

[64] Ratna Debdatta, and J. Karger-Kocsis, 2008, "Recent Advances in Shape Memory Polymers and Composites: a Review," *Journal of Materials Science*, **43** (1), pp. 254-269.

[65] Liu Y., Han C., Tan H., Du X., 2010, "Thermal, Mechanical and Shape Memory Properties of Shape Memory Epoxy Resin," *Materials Science and Engineering: A*, **527** (10) pp. 2510-2514.

[66] May Clayton A., 1987, “Epoxy Resins: Chemistry and Technology (Second edition),” *Marcel Dekker Inc.*

[67] Momentive, 2005, “EPON Resin 826,” *Technical Data Sheet*, Retrieved March 20, 2014 from http://www.momentive.com/Products/TechnicalDataSheet.aspx?id=3937

[68] Huntsman, 2007, “Jeffamine D-230 polyoxypropylenediamine,” *Technical bulletin*, Retrieved March 20, 2014 from http://www.huntsman.com/performance_products/Media%20Library/Jeffamine D-230 polyoxypropylenediamine

[69] Huntsman, 2005, “Epoxy and Jeffamine Polyetheramines,” *Epoxy Formulation Using Jeffamine Polyetheramines Brochure*, Retrieved March 22, 2014 from http://www.huntsman.com/performance_products/Media%20Library/global/files/epoxy_formulations_using_jeffamine_polyetheramines.pdf

[70] Sigma Aldrich, “Neopentyl Glycol Diglycidyl Ether,” *Specification Sheet* Retrieved March 21, 2014 from http://www.sigmaaldrich.com/catalog/product/aldrich/338036?lang=en&region=US

[71] Xie, Tao, 2013, "Method of Fabricating Shape Memory Polymer-Based Three Dimensional Devices," *US Patent 8608999 B2.*

[72] Mooney M., 1940, "A theory of Large Elastic Deformations," *Journal of Applied Phys*ics, **11**, pp. 582-592.

[73] Rivlin RS., 1948, "Large Elastic Deformations of Isotropic Materials," *Philosophical Transactions of the Royal Society A*, **241**, pp. 379-397.